Study of p53 dependent signaling pathways involved in human lymphoma pathogenesis using MS-based proteomics combined with Transmission Electron Microscopy and High Content Imaging

Anna Aspasia Karkavitsa

Supervisor: Assoc. Prof. Michalis Aivaliotis, AUTh/IMBB

MSc Molecular Biology and Biomedicine

Biology Department

University of Crete

Heraklion, Crete Greece

19/10/2018

ACKNOWLEDGEMENTS

I am thankful to my thesis guide Associate Prof. M. Aivaliotis for his guidance, support, encouragement and motivation, and patience throughout the course of this work. I would like to thank the two other thesis committee members: Dr. S. Papamatheakis and Prof. DG. Podikoglou. I am highly thankful to Dr. K. Psatha for her enthusiastic support in the planning of experiments, analysis of the experimental data and scientific interpretation of the results. I am thankful to MSc A. Kalantidou and the other members of the lab members of Aivaliotis Group and Proteomics Facility of IMBB (N. Kountourakis, MSc, Dr. L. Andrianos and Dr. G. Orfanoudaki) for their help at different stages of this work and for providing a friendly environment. I thank Dr. E. Deligianni for the High Content Imaging and the analysis of my samples. I would also like to thank Prof. E. Drakos for providing us the cell lines, Prof. G. Chalepakis, Dr. K. Britakis, E. Papadogiorgaki for the imaging of my samples with the Transmission Electron Microscope, Prof. A. Gravanis and Prof. D. Kardasis and members of his lab for kindly providing us support, while I used equipment in their lab during my experiments. Finally, I would like to thank my family and my boyfriend Alexandros for their never-ending love and support.

Contents

Abstract

The heterogeneity of lymphomas is the major issue that leads to different responses to treatments. Even though the survival rate has increased over the last decades, many patients and particularly elderly people, do not respond to treatments, and in fact the chemotherapy regimens used are not well-tolerated by them. Thus, it is of great need to find new ways for developing new more tolerable and efficient treatments. Nutlin-3a (N3a) is a recently developed small molecule which antagonizes MDM2 and disrupts the interaction between p53 and MDM2. Lymphomas show high percentage of wild type p53 at diagnosis and as a result they are strong candidates for treatment with N3a.The apoptotic effect of N3a was assessed in three lymphoma types (Hodgkin lymphoma, Mantle Cell Lymphoma and Anaplastic Large Cell Lymphoma) using High Content Imaging. High Content Imaging was also used for the study of the mitochondria and their membrane potential deregulation after treatment with N3a. Bionformatics analysis of data from MS-based proteomics revealed that N3a treatment influenced the autophagic pathway. Verification of the proteomics data was achieved using Transmission Electron Microscopy and Western Blots. In addition, an effort was made to study the effect of N3a on NFκB signaling. Finally, our results showed the apoptotic effect of N3a in the three lymphoma types of our study and also indicated a deregulation of the mitochondrion's' membrane potential. They also indicated an increase in the autophagic pathway after treatment with different concentrations of N3a.

1. Introduction

1.1 Lymphoma

Lymphoma is a type of cancer that develops from the white blood cells or lymphocytes. The cells responsible for the occurrence of lymphoma are T, B or NK cells at any stage of their differentiation. Lymphoma affects the lymph nodes and its type depends on the cell of origin. Lymphomas can be divided into two main categories : Hodgkin and Non Hodgkin lymphomas[1].

Hodgkin lymphoma is characterized by few malignant Reed Sternberg cells of B cell origin, which are surrounded by a microenvironment full of T cells, on-malignant B cells, eosinophils and stromal cells[2].

Non-Hodgkin lymphomas comprises all the types of lymphomas except for Hodgkin lymphomas. Most types of Non-Hodgkin lymphomas begin in B lymphocytes.

1.1.1Causes and risk factors

The causes of the occurrence of lymphoma are not yet fully understood. However, there are plenty of possible factors that may put the person at risk of having this disease. Some causes/risk factors are listed below:

1. Immunodeficiency[3]
2. Autoimmune diseases[3]
3. Genetic factors[4]
4. Infectious agents such as Epstein Barr virus[5] and HIV[6]
5. Age[4]
6. Sex[7,8]
7. Exposure to chemicals such as pesticides[9]

1.1.2 Clinical features, diagnosis, staging

Clinical features

In Hodgkin lymphoma the most common symptom is the swelling of the lymph nodes, which are painless and can be felt as rubbery. The cervical and the subcervical lymph nodes are the most commonly affected lymph nodes. The patients can develop other symptoms along with the swollen lymph nodes which include fever, fatigue, short

breath, itching, night sweats and unintended weight loss[7].

In Non-Hodgkin lymphoma except for the swollen lymph nodes, which is still the most common symptom, other symptoms vary depending on their location in the body. Secondary symptoms are the same as Hodgkin's lymphomas in addition to bone and chest pain.

Diagnosis

There are many ways to diagnose a patient with lymphoma, such as:

1. Physical exam during which the doctor will check for swollen lymph nodes and the status of the spleen and liver
2. Biopsy procedure after the removal of a lymph node, in an effort to identify lymphoma cells and their type along with their differentiation stage
3. Bone marrow aspiration to detect whether lymphoma cells are present
4. Many imaging methods such as PET,MRI,CT scan to examine the presence of lymphoma in other areas of the body[10]
5. Additional blood tests to assess the function of the organs and the capability of the patient to undergo chemotherapy

Staging

The staging system, named Ann Arbor, is the same for Hodgkin and Non Hodgkin lymphoma and it consists of the following four (IV) stages.[11]

Stage I: The cancer is isolated in one region such as a lymph node and its surrounding area. Stage I often will not have outward symptoms.

Stage II: The cancer is located in two different regions, an affected lymph node and a secondary region, both regions reside in one side of the diaphragm.

Stage III: Indicates that the cancer is located in both sides of the diaphragm and it includes a lymph node, a secondary region near the lymph nodes or spleen.

Stage IV: Indicates the involvement of other organs that are extralymphatic.

Each stage of lymphoma may also be classified by letter designations. Each of the letters can be appended to some stages:

A or B: the absence of constitutional (B-type) symptoms is marked as "A" to the stage; the presence is marked as "B" to the stage.

S: marks the spread of the disease to the spleen.

E: is used if the disease is "extranodal" (not in the lymph nodes) or has spread from lymph nodes to adjacent tissue.

X: is used if the largest deposit is >10 cm large ("bulky disease"), or whether the mediastinum is wider than ⅓ of the chest on a chest X-ray.

1.2. Types of lymphoma

There are many types and subtypes of lymphoma, both Hodgkin and Non-Hodgkin. For the purpose of this study, only a few will be mentioned, focusing mainly on cHL (nodular sclerosis subtype), MCL and ALK+ALCL.

1.2.1 Classic Hodgkin Lymphoma (cHL)

The main characteristic of classic Hodgkin lymphoma is the presence of a few binuclear Reed Sternberg cells (RS) that are surrounded by an inflammatory microenvironment. In addition, there are mononuclear variants that have cytologic features similar to RS cells. Other cells that can be found in the infiltrate are lacunar and “mummified” cells that obtain dark and condensed chromatin.[8]

1.2.2 Nodular Sclerosis cHL

Nodular Sclerosis is a subtype of classic Hodgkin lymphoma and it is the most common one as it comprises the 50%-80% of the cases and it affects mostly young adults. Bands of collagen fibrosis cause the thickening of the lymph node capsule and the nodal parenchyma is dissected through. The effect of the bands of collagen fibrosis can be observed both macro- and microscopically. Lacunar cells are found in this subtype and they show cytoplasmic retraction. ‘Syncytial variant’ of nodular sclerosis cHL, which are the large aggregates or sheets of neoplastic cells that are surrounded by an inflammatory microenvironment, are observed.[8]

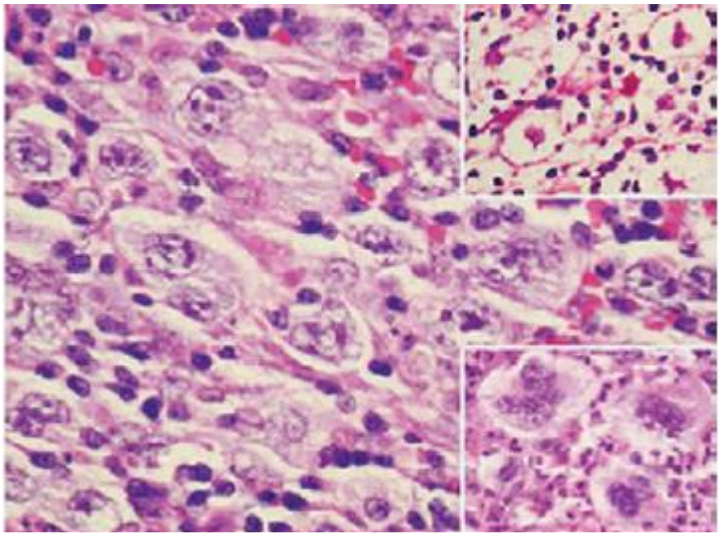

Figure 1.1 Immunohistochemical characteristics of a Nodular Sclerosis Hodgkin lymphoma .Clusters of large neoplastic cells with LP, centroblastic, multinucleated (bottom inset) or lacunar cell-like (top inset) cytologic features. [12]

1.2.3 Mantle Cell Lymphoma (MCL)

Mantle Cell lymphoma (MCL) belongs to the family of Non-Hodgkin lymphomas and it is an aggressive form with poor prognosis. Elderly men at an age of 65-70 tend to be diagnosed with the disease more frequently[13]. MCL is a B cell lymphoma that consists of small to medium sized lymphoid cells with irregular or cleaved nuclei and it bears a CCND1 translocation. It has been hypothesized that the cell of origin is a peripheral naïve pregerminal B cell of the inner mantle zone [14].MCL cells have high expression of monotypic surface immunoglobin, sIgM or IgD and are frequently positive for CD5 and CD43 .Additionally, they express CD19, CD20, CD22, CD79a, CD79b[14].

The most common genetic feature of MCL is the translocation t(11;14)(q13;q32) that juxtaposes CCND1 to the IgH promotor locus and is considered the major event that leads to oncogenesis, as cyclin D1 is overexpressed and it contributes to cell cycle deregulation. In addition, secondary genetic aberrations might affect other molecular pathways, which involve cell proliferation, cell survival and DNA damage response that contribute to the occurrence of the disease. More specifically, upregulated BCR and NFκB signaling play a major role in the occurrence of MCL. Additionally, it has been observed that the PI3K/AKT/mTOR cascade, Notch, Wnt, ARF/MDM2/p53 signaling pathways, along with the overexpression of the antiapoptotic BCL2 protein can lead to MCL lymphomagenesis[13,14].

The treatments of choice available for MCL are chemotherapy (CHOP) along with immunotherapy (rituximab) and targeted therapy with inhibitors of pathways mentioned above, such as mTOR (temsirolimus, ibrutinib, bortezomib).

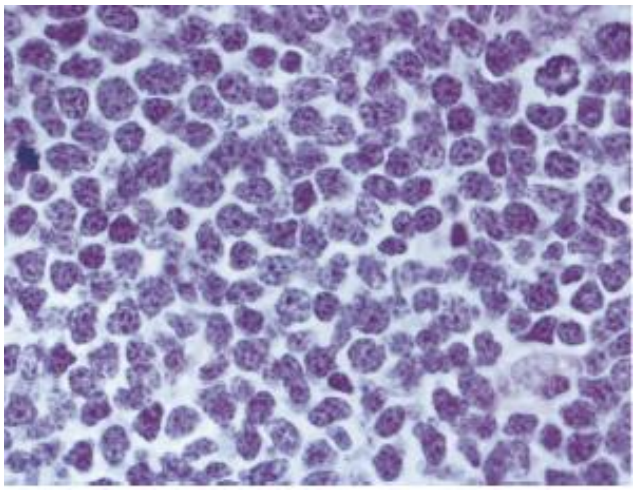

Figure 1.2 Immunohistochemical characteristics of MCL blastoid variant. Mantle zones and the colonized follicles exhibit small to medium size malignant mantle cells with round to slightly irregular nuclei, and scanty cytoplasm [15].

1.2.3 ALK+ Anaplastic Large Cell Lymphoma (ALCL)

ALCL belongs to the group of Non-Hodgkin lymphomas and derives from cytotoxic T cells. ALCL comprises 3% of adult and 10% - 20% of childhood non-Hodgkin lymphomas and is most frequent in the first 3 decades of life[16]. The cells are large with abundant cytoplasm and 'bean-shaped' or horse-shoe- shaped' nuclei with multiple nucleoli that are more prominent, and scattered chromatin[17]. ALK(+)-ALCL is a subtype of ALCL characterized by characterized by strong CD30 immunostaining and recurrent chromosomal translocations involving the ALK gene, in which the Anaplastic lymphoma kinase (ALK) on chromosome 2 fuses with the nuclephosmin (NPM) in chromosome 5. As a result, a chimeric protein is formed, NPM-ALK, which has constitutive tyrosine kinase activity[18]. It should also be mentioned that ALK(+) ALCL is positive for CD2,CD5,CD4,CD45,CD25,CD61 immunostaining[16].

The genomic breakpoints which are involved in ALK translocations are located in the intron that is between 16 and 17 exons. The translocation results to the fusion of a 5

end partner with the 3 end ALK tyrosine kinase domain. The new domains provided by the 5 end partner allow the dimerization and holo-, heterocomplex creation. These complexes allow the fusion kinase to phosphorylate itself, but also phosphorylate and interact with other proteins as well[19]. The localization of the chimeric protein is important as the wrong compartmentalization could affect the cell homeostasis. In the case of ALK:NPM1,the NPM1 is responsible for the expression of a protein that is involved in multiple pathways, such as ribosome biogenesis, transport of pre-ribosomal particles, genomic stability(through p53 regulation) and transcription. NPM can act as an oncogene or as a tumor suppressor according to its level of expression. It has been proposed that the wrong compartmentalization of ALK:NPM results in the formation of complexes with NPM and might be the cause for the many genetic aberrations observed in ALCL[20].

In ALK+ ALCL, a relationship between CD30 and ALK exists[21] and activates the NFκB pathways, leading to apoptosis and p21 mediated cell cycle arrest. Other signaling pathways that are affected in this type of lymphoma are JAK-STAT3 and PI3K-AKT pathways[17].

ALK+ALCL treatments involve primarily chemotherapy (CHOP), targeted molecular therapy (anti-CD30[22], anti-ALK) and vaccination against ALK[17].

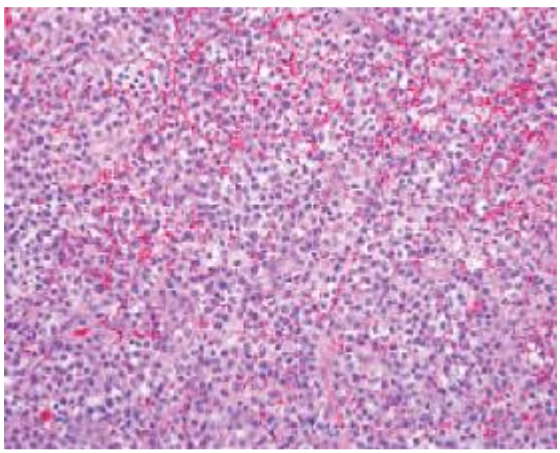

Figure1.3 Immunohistochemical characteristic of ALCL. The cells are positive for anaplastic lymphoma kinase with nuclear and cytoplasmic positivity [23]

2.1 p53 tumor suppressor pathway

p53 is a transcription factor that is stimulated by cell stress conditions, such as DNA damage, signals from oncogenes that promote cell growth, hypoxia and metabolic alterations. When p53 is activated, it tetramerizes and through its transcriptional activities it regulates various cellular processes, such as autophagy, metabolic changes, cell cycle arrest or senescence, DNA repair and apoptosis induction[24].

p53 can control and induce apoptosis both transcriptionally and through processes that don not involve its transcriptional activity. Transcriptionally, p53 can upregulate the pro-apoptotic mitochondrial protein Bax, pro-apoptotic BH3 proteins, such as Puma and Noxa, but also death receptors of the extrinsic apoptotic pathway (CD95,TRAIL-R2)[25]. In a non-transcriptional manner, p53 through its DNA binding domain, interacts and neutralizes the Bcl-2 and Bcl-K_L's anti-apoptotic functions and subsequently activates the pro-apoptotic BH3 proteins Bax and Bak.This results into the permeabilization of the mitochondrial membrane and leads to apoptosis[26].

2.2 Regulation of p53

The rate of p53's degradation is the main factor that determines its stability, and under normal conditions the half-life of p53 is less than thirty minutes. MDM2 is an E3 p53 specific ubiquitin ligase that regulates p53 degradation via proteasomes. In addition, the transactivation domain of p53 is blocked by MDM2 and as a result p53 is exported to the cytoplasm for proteasome mediated degradation. An autoregulatory feedback loop between p53 and MDM2 exists as MDM2 is a direct transcriptional target of p53. Another possible regulator of p53 is MDMX (or MDM4) as it can inhibit p53's transactivation domain, leaving the levels of p53 protein stable[24,27]. In response to cellular stress,p53 undergoes modifications, such as phosphorylation at multiple sites, and as a result its interaction with MDM2 is disrupted[28].

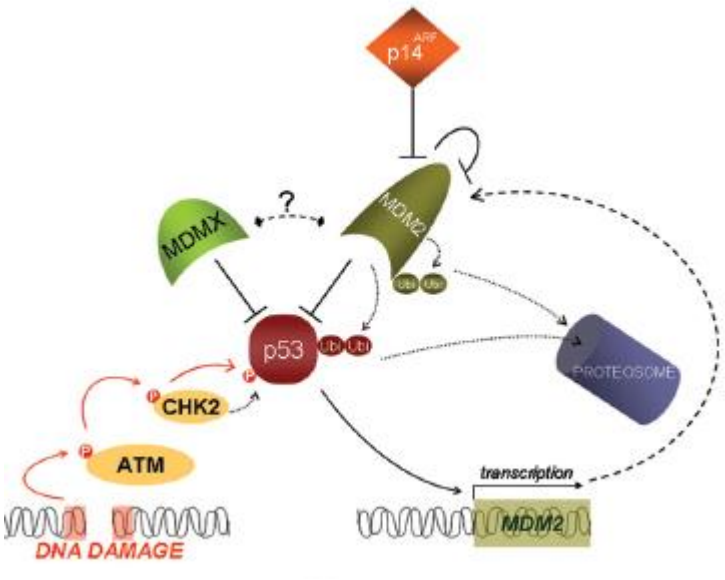

Figure 1.4. Regulation of p53 by MDMX and MDM2 through proteasome degradation [22]

2.3 Targeted activation of p53 through novel strategy using Nutlins

The restoration of p53 in cancer cells is of high importance, since in most cancer types, the function of p53 is inactivated. Although many efforts have been made, such as the use of oligonucleotides to reduce the high levels of MDM2[29], a novel approach has emerged and it focuses on the disruption of the interaction between MDM2 and p53. Their interaction includes four hydrophobic residues (Phe19, Leu22, Trp23, Leu26) in a amphipathic helix that is formed by p53 and a hydrophobic pocket in MDM2[30]. A class of cis- imidazoline compounds, which were discovered by the group of Vassilev and they were named Nutlins, have the ability to disrupt this interaction. The most potent of these cis- imidazoline agents was Nutlin-3a (N3a),which has the ability to displace p53 from MDM2 and stabilize but also activate the p53 pathway[31]. Nutlin-3a can penetrate the cell membrane and through its action, it can induce cell cycle arrest and apoptosis in the range of 1-3μM.

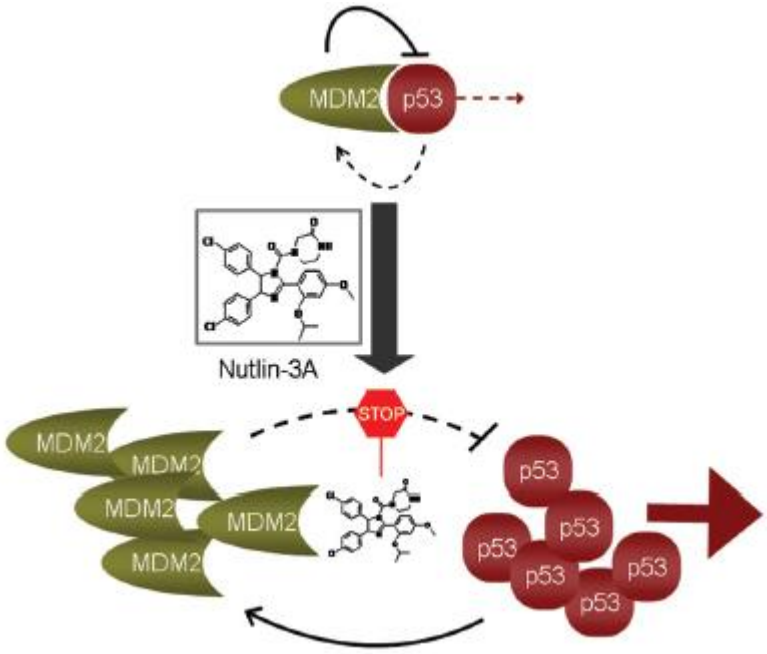

Figure 1.5. N3a's mechanism of action[22].

Although MDM2 and MDM4 p53 binding domains have high homology,N3a does not seem to block the MDM4-p53 interaction[32].However,N3a may regulate the MDM4 levels indirectly, as it increases the levels of MDM2 though p53 activation and promotes the MDM4 degradation since MDM2 plays a significant role in MDM4 degradation[33].

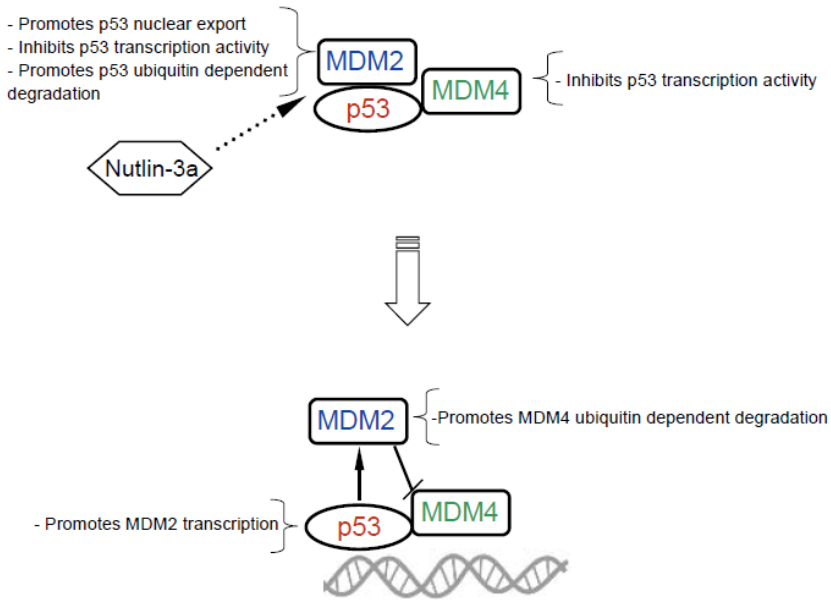

Figure 1.6 Autoregulatory feedback loop between p53 and MDM2 after activation of p53 by N3a[34].

Adult leukemias and lymphomas show high percentage of wild type p53 since low portion of the cases show deleted and or mutated p53 at diagnosis[3536]. As a result, haematological malignancies are a strong candidate for treatment with N3a. In fact, there are several studies that demonstrate the cytotoxic effect of N3a on this type of cancer. Besides the effect of N3a through the transcriptional program of p53, there is evidence that N3a has an effect on apoptosis in a non-transcriptional manner. More specifically, N3a can lead to accumulation of mono-ubiquinated cytoplasmic p53 and rapid translocation to mitochondria. N3a is proven not to interfere with the ability of MDM2 to mono-ubiquinate p53.The translocation of p53 to the mitochondria associates with the cytochrome c release along with the transcriptional activation of p53 target genes. As a result, N3a can induce apoptosis through both transcriptional and non-transcriptional dependent pathways, as it is shown in Fig 1.7.

RG7112 is a compound that belongs to the Nutlin family and has successfully granted permission for a Phase I trial for treatment in acute and chronic leukemias. RG7172 is distributed orally and indeed showed activation pf p53 target genes and complete remissions in cases with poor prognosis. RG7112 also demonstrated effects in patients with chronic leukemias. It should be noted that side effects do exist and include nausea, vomiting and diarrhea. Finally although RG7112 demonstrated activity as a monotherapy in AML cases, the future development of MDM2 antagonists for treatment will require combinational therapies[37].

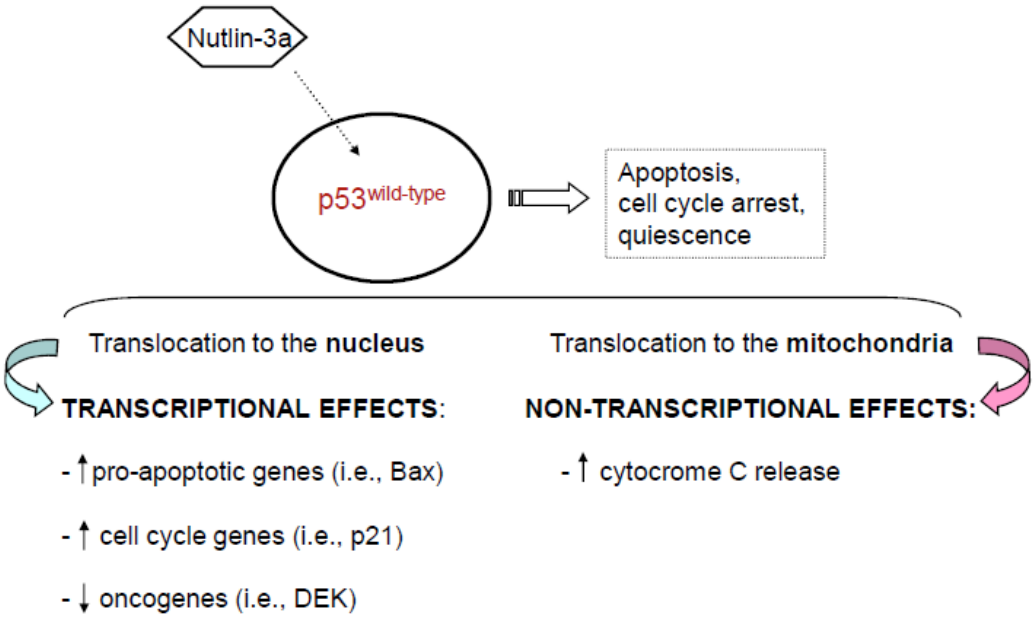

Figure1.7 Effects of N3a both in a transcriptional and non-transcriptional manner[34].

3.Signaling pathways affected in lymphomagenesis

3.1.1. Autophagy

Autophagy is a process that contributes to cytoprotection, it is induced upon intracellular and extracellular stress stimuli and leads to the degradation of cytoplasmic components and organelles by lysosomes and their subsequent recycling. Autophagy is associated with various physiological functions, such as haematopoiesis and immune responses. In haematological malignancies, autophagy can either contribute to chemotherapy resistance or to the suppression of the tumor depending on the context.

3.1.2 Autophagic machinery

Firstly, the isolation membrane named “phagopore” is formed and it is promoted by two mechanisms, after energy, growth factor or nutrient deprivation. One mechanism relies on the inhibition of mTORC1 (mTOR ,Raptor, MLST8, PRAS40, DEPTOR)[38], which consists of mTOR and Raptor and inhibits autophagy by phosphorylating ULK proteins. Under conditions of nutrient and growth factor deprivation, mTORC1 becomes inactive and dissociated form ULK1/2, allowing its dephosphorylation and subsequent activation. The second mechanism involves the direct phosphorylation/activation of ULK1 by AMPK, which allows ULK1/2 to form the autophagosome by regulating the Beclin-1 interactome. Beclin-1 complex consists of Beclin-1, PI3K, Vps34, Vps15 and

AMBRA1 and its activity is essential as it activatesVps34 lipid kinase, which is important for autophagy. Atg12 and Atg8/LC3 are two ubiquitin-like protein conjugation systems which are also important for autophagosome formation. Atg12 complexes with Atg5 and along with Atg10 and Atg7 promote the phagosome nucleation. Lipid phosphatidylethanolamine (PE) is conjugated to mammalian LC3-I through the Atg8/LC3 conjugation system and converts LC3-I to a more soluble form (LC3-II), which can associate with the autophagosome membrane. Many proteins interact with LC3-II, such as p62/SQSTM1 though their LIR domain (LC3-interacting region) and their role is to target structures, such as mitochondria, endoplasmic reticulum, etc. to the autophagosomes. When the autophagosomes are matured, they interact with Rab7+ endosomes to create amphisomes. Finally, amphisomes fuse with lysosomes to create autophagolysosomes in order to be able to degrade their content and release it to the cytosol[39].

3.1.3 Regulation of autophagy

Autophagy is regulated by many factors during various steps of the procedure. The association of Beclin-1 with PI3K is inhibited by Bcl-2 and Bcl-X_L and as result autophagosome membrane nucleation does not occur. Another pathway that inhibits autophagy is the mTOR and especially mTORC1 complex. The mTORC1 complex inhibits autophagy by unifying signals generated by growth factors, energy depletion, hypoxia and DNA damage. PI3K/Akt signaling cascade is capable of controlling mTORC1. PI3K is activated after insulin and other growth factor signals and phosphorylates and activates Akt. Subsequently, Akt phosphorylates and inhibits TSC2 (tuberin) which along with TSC1 forms the TSC complex and activates the mTORC1.After the activation of mTORC1, autophagy is inhibited as UKL1 is phosphorylated and inactivated. A decrease of the intracellular ATP:AMP, which is under normal conditions high, results into the activation of AMPK which is a positive regulator of autophagy as it inhibits the mTORC1[40]. P53 also plays a complex role in regulating autophagy, since the nuclear p53,using its transactivation ability, activates mTORC1 inhibitors and metabolic genes, while cytoplasmic p53 activates the mTOR pathway leading to the inhibition of autophagy[41].

3.1.4 Autophagy in lymphomagenesis

Autophagy may influence the initiation and the progression of cancer but also play an important role in the effectiveness of the therapeutic strategies used to treat the disease[42].On one hand, autophagy can be a safety net against tumorigenesis in the early stages of tumor development, as it safeguards against metabolic stress through proper function of mitochondria and through clearance of protein aggregates. Metabolic stress and pro-inflammatory stimuli, along with the deletion of autophagy genes, may contribute to genomic instability due to DNA damage. On the other hand, autophagy assists the survival of established tumors, as it can help them to cope with nutrient and energy starvation along with hypoxic conditions and cancer therapies. This is achieved though generating 'dormant' cells, which can resume and proliferate when the conditions are more favourable[43]. Thus, autophagy may act as an obstacle in successful cancer therapies. Studies with Beclin-1 and Atg5 set an example on how the role of autophagy in haematological malignancies is context dependent. Beclin-1 heterozygous mice resulted into reduced autophagy, elevated cell proliferation and lymphomagenesis[44]. Low expression of Atg5[45] or Atg5 haploinsufficiency[46] is associated with the promotion of lymphoid malignancies. However, knockdowns of Beclin-1 and Atg5, along with the use of the antimalarial drug chloroquine (CQ) sensitized leukemia cell lines in TRAIL-mediated apoptosis. In addition, the use of shAtg5 assisted the cell death induced by alkylating drug therapy[47].

3.2.1 NFκB signaling pathway

NFκB is a family of inducible transcriptional factors that are important in the activation and survival of immune cells. The mammalian members of this family are RelA (p65), RelB, c-Rel, NFκB1 (p50 and its precursor p105) and NFκB2(p52 and its precursor p100). The activation of NFκB relies either on the canonical or the non-canonical pathway. The canonical pathway is activated through pro-inflammatory cytokines (IL-1,TNF-a), PAMPS attached to TLRs, T cell receptor signaling cell receptor signaling and lymphocyte co-receptors (CD30, CD40)[48–50]. The canonical pathway is dependent on the action of the RelA/p50 subunits, which under normal conditions reside in the cytoplasm and are inhibited by IκBα. Upon cell stimulation, IκBα is phosphorylated by the IKK complex, which consists of IKKα, IKKβ and IKKγ (NEMO) and is degraded by ubiquitin mediated proteasome activity. Subsequently, the RelA/p50 dimer is free to

translocate in the nucleus in its active form to transcribe the target genes[51].The non-canonical pathway is activated through the association of RelB subunit with p50 or p52.BAFF,CD40L,LTβ and RANKL are the ligands that are responsible for the activation of this pathway[49]. NIK activates IKKα which causes the degradation of p100,which is the precursor of p52.Under normal conditions, RelB resides in the cytoplasm in the complexes of RelB/p100 or RelB/p50/p100 and after the degradation of p100 the remaining of the complexes can translocate to the nucleus for the transcription of the target genes[52].

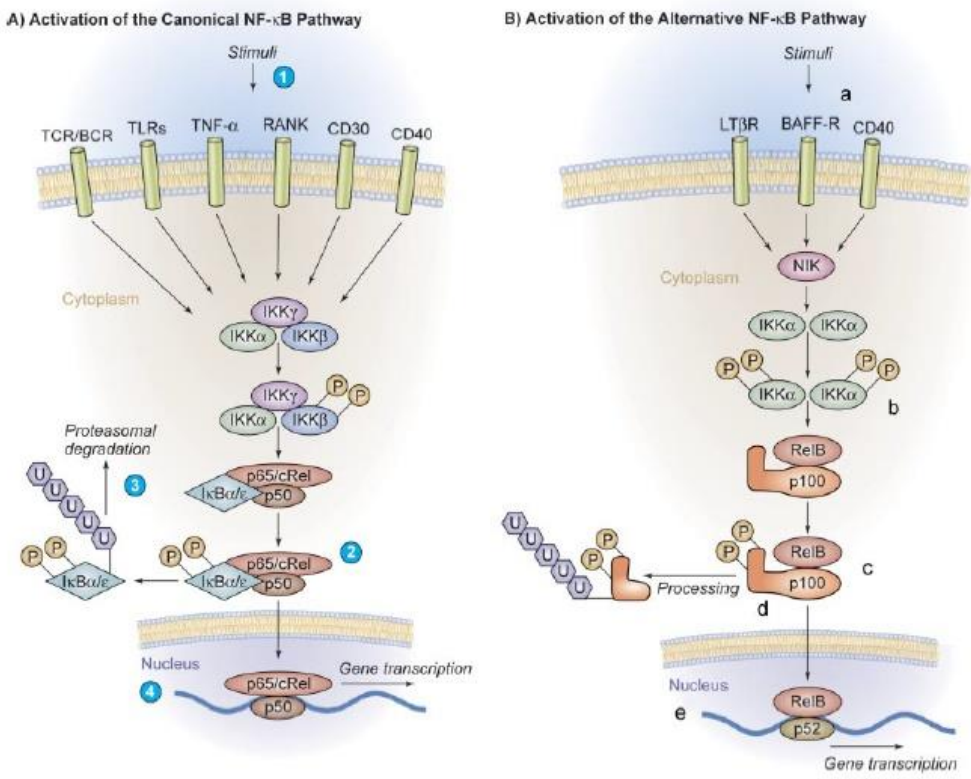

Figure 1.8. NFκB signaling pathways. (A) The canonical signaling pathway, (B) the non-canonical signaling pathway[50].

3.2.2 NFκB signaling in lymphomagenesis

Deregulation of NFκB signaling pathway can initiate or sustain many types of cancer. In particular, oncogenic mutations, translocations and other alterations affecting this signaling pathway are frequently observed in B cell malignancies, as this pathway is very important for normal B cells. These genetic aberrations may lead cancer cell and tumors addicted to NFκB signaling.

In Hodgkin lymphoma cell lines and HRS cells a constitutive accumulation of NFκB heterodimers in the nucleus is often observed[53]. Truncating mutations in IKBα have also been discovered in Hodgkin lymphoma cell lines[54,55]. HRS cells show high expression of many TNF receptor family members, such as CD30[56], CD40[57], RANK[58], which can be chronically stimulated by the inputs of the HRS cells' reactive microenvironment or by HRS cells themselves. In Epstein–Barr virus-associated (EBV), and through the EBV encoded protein LMP1 the canonical and the non-canonical NFκB pathways are activated[59]. Frameshift or nonsense mutations in the gene encoding IKBα result into inactive shortened isoforms of IKBα[54,60]. Finally, TNFAIP3 gene which encodes a protein that is a negative regulator of NF-κB, is observed in 20% lymphoma cases and especially in EBV-negative cHL. ALCL is also characterized by constitutive activation of the canonical and non-canonical pathways by overexpression of CD30[51]. The BCR-NF-κB activation plays an important role in the molecular pathogenesis of MCL as overexpression of SYK has been observed. In addition, activating mutation occur in the coiled coil domain of CARD11 in relapsing tumors and lead to the activation of NFκB canonical pathway[13]. In summary, in a variety of lymphoma cases, NFκB signaling is upregulated and promotes cell survival and proliferation and thus this pathway is one of the best targets for therapy.

4.1 MS-based proteomics for the study of lymphoma

As it was mentioned above, lymphomas have many proteins and signaling pathways deregulated and altered during lymphomagenesis, but also after treatments. Profiling of the proteins, their modifications but also their interactions though MS-based proteomics and bioinformatics can be of great assistance in the study of lymphoma pathogenesis. MS-based proteomics have the ability to bridge basic research and clinical application through personalized medicine. Through MS-based proteomics, quantitation of selected peptides, interaction between proteins, location of the proteins and study of the changes in the proteome after drug therapy, can be performed. Using this approach, we extract information about the differences between healthy and lymphoma cells, lymphoma subtypes and also about the differences between treated and non-treated lymphoma cells. Finally, discovering biomarkers for early diagnosis and prognosis is of high importance for the use of MS

based proteomics in clinical application[61].

Scope of the study

Three lymphoma cell lines representing both Hodgkin and Non-Hodgkin lymphomas will be subjected to treatments with a cis-imidazole compound named Nutliln-3a. Nutlin-3a is capable of non-genotoxic activation of p53 by disrupting the MDM2-p53 binding. Previous work done by the Aivaliotis research group assessed the function of Nutlin-3a by verifying the activation of p53 and also determined the desirable concentrations to use in treatment assays[62]. The present study is based on these previous data and uses them to study the effects of the non-genotoxic activation of p53 by Nutlin-3a and its effect on cell death, autophagic pathway and NFκB signaling.

2. Materials and methods

2.1 Cell culture

Cell culture is the procedure by which cells are grown under controlled conditions and not in their natural environment. The conditions under which cells are grown are specific for each cell type. Most cells require a solid substrate, in order to grow (adherent cells) whereas others can be grown without it (suspension culture). It is important to highlight that frequently cell lines are used for cell culture and the study of many diseases.

A cell line is a population of cells which has derived from one single cell and contain the same genetic makeup. Frequently, such cells are mutated evading normal cellular senescence and continue to proliferate unimpeded. This ongoing proliferation results in the production of an immortalized cell line.

2.2 Cell lines

Three lymphoma cell lines were cultured and used for experiments for the purpose of this thesis. Two of the three cell lines were Non-Hodgkin lymphoma, whereas the other one was classic Hodgkin lymphoma. These cell lines were kindly provided to our lab by Dr. E. Drakos and his colleagues from the University of Texas MD Anderson Cancer Center, Houston, TX, USA.

Lymphoma's Classification	**Lymhoma subtype**	**Origin**	**Genotype**	**Named cell lines**
HL	HL	preapoptotic GC B cells	B-cell	MDA-V
NHL	MCL	blastoid variant of MCL, pre-GC B cells of the mantle zone		JMP-1 (M-1)
	ALCLALK+	T- or null-cell lineage	T-cell	SUP-M2

Table 1. Cell lines used for this thesis

MDA-V: These B cells belong to classic Hodgkin lymphoma type (cHL). The cells were isolated from the lymph nodes of a 45 year old untreated male patient with EBV-positive, who was diagnosed with stage I classic Hodgkin lymphoma with nodular sclerosis[12].

JMP-1: These B cells are classified as a blastoid variant of MCL, a rare Non-Hodgkin lymphoma type. This cell line derived from a 58 years old man's peripheral blood with relapsing mantle cell lymphoma. Originally, the patient was diagnosed with blastoid MCL in leukemic phase and harbored the chromosomal rearrangement t (11; 14) (q13; q32)[63].

SUPM-2: This cell line is comprised of T cells deriving from the cerebrospinal fluid of a 5-year-old girl with refractory malignant histiocytosis and is classified as Non-Hodgkin lymphoma type. The cells are positive for the mutation of NPM-ALK, express CD30, defining the cells as anaplastic large cell lymphoma (ALCL)[64].

2.3 Culture medium- growth conditions

The lymphocyte cell lines used for this thesis were handled under aseptic conditions and under the strict rules that a cell culture requires. Their handling for passaging and treatments was done inside a laminar flow cabinet. The cabinet and the tools inside it were disinfected with 70% ethanol prior to their use, to ensure aseptic conditions and prevent any possible contamination.

The growth conditions of the lymphocyte cell lines were determined by previous members of the lab. The cells were obtained from previously cryogenically stored respective cell lines, which were conditioned in liquid nitrogen and then they were cultured in $25cm^2$ and $75cm^2$ flasks.

The cell density where the cells were grown was 10^6cells/ml in a specific culture medium. The consistency of the culture medium was:

1. RPMI 1640
2. 15% Fetal Bovine Serum (FBS)
3. 1% Penicillin/Streptomycin

It has to be noted that the FBS was heat inactivated (30 minutes at 56^{0C}), aliquoted in 50ml falcons and then stored at -20°C for future use. All items were purchased by Thermoscientific Gibco.

2.4 Subculture of cells

The flasks (Corning.Inc) were stored in a humidified atmosphere containing 5% $C0_2$ and its temperature was steady at 37°C. The observation of the cells under a brightfield microscope was a critical and a necessary step before any further experimental handling. The observation of the cells allows to determine, along with other methods, their morphology, concentration and whether a bacterial contamination had occurred. The following protocol describes the general procedure that was followed to subculture the cells.

Experimental procedure.

1. Culture medium (previously stored at 4°C) was prewarmed in a 37^0C waterbath.
2. Cells were collected from the flasks
3. Small amount of cells was kept for Trypan Blue Assay to determine cell viability
4. Cells were centrifuged at 1000 rpm for 5 min, RT
5. The supernatant of the cells was aspirated
6. Cell pellet was resuspended with the appropriate amount of fresh prewarmed culture medium at a density of 10^6 cells per ml

2.5 Freezing of cells

Cell lines were cryopreserved in liquid nitrogen and stored at -80°C at a controlled rate. When the viability of the cells was over 90%, a cryovial was created to ensure their perpetuation (6-10x10^6 cells/ml; 1,5 ml/vial). The synthesis of the freezing medium used for this process is described below.

Freezing Medium

1. Culture medium (RPMI 1640 with 15%FBS and 1% pen/strep) 60% (Gibco))
2. Heat inactivated FBS 30%
3. Dimethyl sulfoxide (DMSO) 10% (Applichem)

DMSO was added to prevent the formation of intracellular ice crystals during the freezing process, protecting cells from frozen cell injuries. However, it is important to note that DMSO is toxic to the cells at room temperature, emphasizing the need to begin cryopreservation quickly thereafter.

Experimental procedure

After reculture procedure was completed the following steps occurred:

1. Labelling of the cryovials with the name of the cell line, date of freezing and cell number
2. Centrifugation of cells at 1000 rpm for 5 min, RT
3. Aspiration of the supernatant
4. Resuspension of the cells in 1,5ml of freezing medium
5. Temporary cell storage at -20^{o}C for 15 min before their permanent storage at -80^{o}C or in liquid nitrogen

2.6 Thawing of cells

Thawing of the cells requires quick handling (< 1 minute), in order to minimize the toxic effects of DMSO. The following protocol describes the general procedure that was followed for thawing the cryopreserved cells of our study.

Experimental procedure

1. Remove the cryovial from the refrigerator or the liquid nitrogen
2. Place the cryovial inside the incubator (37^{oC})
3. When the ice is just a small bit left in the vial, transfer it into the laminar flow hood.
4. Gently, transfer the desired amount of pre-warmed complete growth medium dropwise into a 15ml falcon containing the thawed cells
5. Centrifuge at 1000rpm for 5min, RT
6. Aspirate supernatant
7. Resuspend cells in 3ml of fresh prewarmed culture medium
8. Seed cells in a 25cm^2 flask

2.7 Trypan Blue viability test

Trypan Blue viability test is an assay used to determine the viability of the cells. Trypan Blue viability test relies on the Trypan Blue azo dye, which has the ability to dye dead cells blue whereas live cells remain unstained. This is based on the fact that the membrane of the dead cells has lost its ability to be selective and as a result the dye can pass through and stain them, whereas live cells remain unstained[65]. This assay takes place in a Neubauer chamber, which is s a thick glass plate with the size of a glass slide (30x70x4mm). The ruled area consists of 9 large squares with 1mm^2 area as it is shown on the image below.

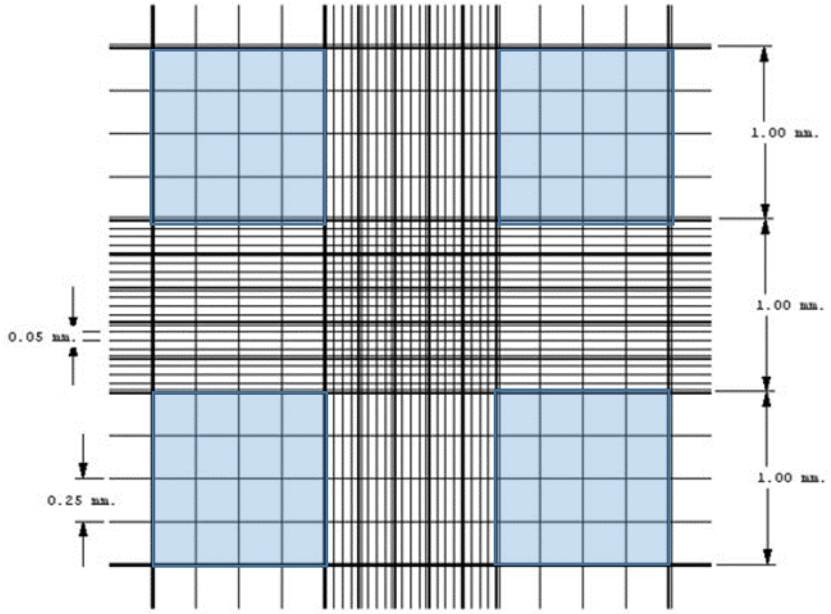

Image 2.1. Representation of the Neubauer chamber and the spaces in which White Blood cells are counted (blue squares)[66].

The following protocol describes the general procedure that was followed to assess the cells viability

<u>Experimental procedure</u>

1. Collect cell sample from the flask during reculture, ensuring cells are evenly distributed.
2. Mix gently 10µl of the sample with 10µl of Trypan Blue dye (1:1 dilution)
3. Careful place the dilution of the cell suspension with the TB solution into the well of the Neubauer counting chamber underneath the coverslip

4. Observe under a phase contrast optical microscope with a 20X objective
5. Using a hand tally counter, count cells (stained/unstained) according to Image 1.2. Calculate the percentage cell viability and the number of viable cells/mL in the original cell suspension, taking the average cell count recorded for each of the 16 corner squares, according to the equation below:

% Cell viability = (# alive cells/ # total cells)*100

Concentration of the cells/ml = #alive cells*dilution of the dye*10^4 (the physical dimensions of the Neubauer)

2.8 Cell lysis

Cell pellets from each cell line were obtained from cells with viability over 90% and in log-phase growth. The following protocol describes the general procedure that was followed to achieve cell lysis.

Experimental procedure

1. Centrifugation of cells for 5 min in 1000 rpm
2. Aspiration of the supernatant
3. Redilution in 1xPBS
4. Centrifugation of the sample for 5min in 1000rpm
5. Aspiration of the supernatant
6. Preparation of the cell lysis buffer

   Per 1ml Lysis Buffer add:

   - PMSF (1 mM)
   - DTT (1 mM)
   - phosphatase inhibitors (cocktail I: cocktail II; 1:1)
   - protease inhibitors, according to manufacturer's recommendations (Sigma)
7. Redilution of the cell pellet in lysis buffer according to its size (60µl-200µl)
8. Transfer of the rediluted sample in new 1,5ml tubes
9. Vortex for 10 seconds and sonication of the samples for 60 seconds/30 seconds rest for each cycle

10. Shake the samples for 20 minutes at 4$^{oC.}$
11. Centrifugation for 15 min in 14000 rpm
12. Recollection of the supernatant and placement in new tubes
13. Storage in -80^{oC} for future use or in ice for protein concentration measurement

Joe's lysis buffer

Reagents (Stock)	**Volume per 50 mL of solution (v/v)**	**Final concentration**
0.5M Hepes, pH7.7	2.5 mL	25 mM Hepes
5M NaCl	4 mL	400 mM NaCL
0.5M $MgCl_2$	0.15mL	1.5 mM $MgCl_2$
0.5M EDTA	0.2 mL	2 mM EDTA
10% Triton X100	2.5 mL	0.5% **(v/v)** Triton X100
ddH2O	40.65 mL	

Table 2. Ingredients used for Joe's lysis buffer.

2.9 Bradford assay

Bradford assay is a colorimetric method used, in order to determine the protein concentration of samples. It is based on the capability of proteins to react with the dye Coomassie Brilliant Blue G 250 in acidic aqueous solutions[67].

Experimental procedure

(The following described below is an adaptation of the Bradford method that we used for a 96 well plate format.)

1. Dilute the 5x Bradford reagent with dd H_20 (1:5)
2. Prepare solutions with known BSA concentration (0, 250, 500, 750, 1000 μg/ml) for the formation of the standard curve
3. Dilute 2μl of each sample in 200μl Bradford reagent
4. Plate the samples in triplicates in an ELISA 96 well plate

5. Set the ELISA reader at the wavelength of 595nm
6. Use the average of the three measurements per sample
7. Use the results to graph the standard curve and use the curve and the data from the Bradford assay to determine the unknown protein concentration

2.10 Western Blotting

Western Blotting is a method used to separate and identify proteins. By using this technique, proteins are separated based on their molecular weight through gel electrophoresis and subsequently transferred to a membrane. This membrane will be incubated with antibodies specific for the proteins of interest[68].The following protocol describes the general procedure that was followed to perform a Western Blot.

1. Prepare Lysates from cell lines as it was described in paragraph 2.8 and store at -80^0 C.

2. Prepare the gels (6%, 8%, 12% or 15% polyacrylamide) using the Biorad gel cast, glasses, combs and spacers. Gels can be prepared previously and stored at 4^0C covered by saran wrap.

<u>Gel Electrophoresis:</u>

1. Place the gels to electrophoresis apparatus and rinse with electrophoresis buffer using a syringe. Remove combs. Load preheated lysates with loading/sample buffer (heating plate at 70^0C, 15' or 90^0C, 5') in wells. Set up the power supply at constant V: 60-80V (stacking gel);100V-120V (running gel) (run 1 gel ~1 hr)

<u>WB transfer:</u>

1. Prepare Wet transfer apparatus (BIORAD)
2. Remove the gel(s) from glasses, place in container and wash them in 1X protein Transfer Buffer for 20' on a shaker
3. Place 4 sponges/whatman paper (9X6 cm) in a different container with same buffer. Soak for 10'.

4. Cut the PVDF membrane (9X6 cm), label front right upper corner with a pencil (experiment/date/% gel) and prewet in 100% methanol for 1'. Wash X2 in ddH20 for 2' each. Equilibrate membrane in protein 1X Transfer Buffer for 10'.
5. Protein transfer using the WET method/Assemble the "sandwich": Place the prewet whatman paper, membrane and gel in order, removing carefully any air bubbles (- Black Grid/Sponge/Whatman paper/Gel/Membrane/Whatman paper/Sponge/White Grid +).
6. Set up the power supply at constant mA, 350-400mA, 90-120', in a bucket of ice, in cold room.
7. Remove membrane, mark Markers' MW bands with a pencil.
8. Rinse the membrane with 2 changes of Tween 20 in TBS (0.1% (v/v) TBS-T) and then wash the membrane in TBS for 15' at RT.
9. Block non-specific binding sites by immersing the membrane in 5% (w/v) non-fat dried milk, 0.1% (v/v) TBS-T, 20'-1hr. Briefly rinse w/ TBS-T to remove traces of milk.
10. Incubate the membrane with the determined dilution of primary antibody, 5% milk in TBS-T or 1-5% BSA (between 1:100 – 1:1000), o/n at 4^0 C on a shaker
11. Briefly rinse in TBS-T. Wash with TBS-T, 3X10'
12. Incubate with the determined secondary antibody (anti-mouse or anti-rabbit) at a dilution according to manufacturer's recommendations in TBS-T, 1hr, RT.
13. Briefly rinse in TBS-T. Wash with excess TBS-T, 3X10'.

Chemiluminescence detection:

1. Place the membranes on saran wrap and apply the ECL reagent-mixture for 4-5', according to manufacturer's recommendations. Tilt membranes and pour off excess liquid. Put the membranes in the Chemi-Doc tray.
2. Expose using multiple exposures of 15''or 30''→5'→20' to determine the optimum exposure time for each Ab.
3. Use Chemiluminescence setting on ChemiDoc software to visualize.

Stripping & reprobing:

1. wash w/ TBS-T, 3X10'
2. add the designated stripping buffer (Pierce) (10ml/membrane) & incubate for 20'- 40'
3. wash w/ TBS-T, 3X10'
4. continue immunodetection of other proteins of interest on the same blot (max 3 Abs/blot+ actin) w/ "blocking non- specific binding sites" step

Antibodies: All antibodies were purchased by Santa Cruz except for anti-actin (Merck Millipore) and secondary antibodies (Cell Signaling).

2.11 Cell apoptosis detection using Annexin V and High Content Imaging

During apoptosis there is a loss of membrane phospholipid asymmetry, and as a result phosphatidylserine is exposed at the cell surface. Fluorescein isothiocyanate labeled annexin V has the ability to bind to phosphatidylserine and in this way, through flow cytometry or High Content Imaging, it is possible to detect apoptotic cells[69]. The following protocol describes the general procedure that was followed to stain the cells with Annexin V.

1st day

- Plate 800.000 cells/ml in a 24 well plate
- Use 5μM of Nutlin-3a (10mM) for the treatment
- Use same amount of DMSO for the control cells

2nd day

1. Harvest cells
2. Perform three Trypan Blue counts (viability and cell concentration)
3. Centrifuge at 1000rpm for 5min, RT
4. Resuspension of the cells to obtain 800.000 cells/ml
5. Arrange and name the 1,5ml tubes
   (1) BLANK
   (2) BLANK +PI
   (3) BLANK + Annexin
   (4) Control +PI + Annexin

(5) N3a +PI +Annexin

6. 800.000 cells per tube
7. Centrifuge in 1000rpm for 5min, RT
8. Resuspend in 500-1000μl of 1xPBS
9. Repeat 7,8 steps
10. Resuspend cells in 300μl 1xBinding Buffer (BB)
11. Add 1-2μl/100μl of annexin in samples (3), (4), (5)
12. Incubation in RT for 15 minutes in darkness
13. Add 900μl of 1xBB in samples 3,4,5
14. Centrifuge 1000rpm for 5min, RT
15. Resuspension of the samples (3), (4), (5) in 300μl of 1xBB
16. Add 15μl of PI in samples 2,4,5
17. Transfer samples in a black 96-well plate
18. Add 1:500 Hoescht dye (1μl/100μl of sample)

2.12 Mitochondrial membrane potential using Mitotracker and JC-1 dye

JC-1 and Mitotracker Red CM-H2XRos are used to measure the membrane potential as depolarization of mitochondrial membrane potential is a pivotal step for apoptosis. release of cytochrome c

JC-1 dye is membrane permeant and is widely used in apoptosis studies to monitor mitochondrial health. JC-1 dye exhibits potential-dependent accumulation in mitochondria, indicated by a fluorescence emission shift from green (~529 nm) to red (~590 nm). Consequently, mitochondrial depolarization is indicated by a decrease in the red/green fluorescence intensity ratio[70].

Mitotracker RedCM-H2Xros is a mitochondrial specific dye which is a reduced, nonfluorescent version of MitoTracker Red that fluoresces upon oxidation. This dye also stains mitochondria in live cells and its accumulation is dependent upon membrane potential. In apoptotic cells, the H2-CMX-Ros dye is found to be diffusely distributed in the cytoplasm because depolarized mitochondria cannot retain this dye[71].In addition, Mitotracker RedCM-H2Xros is also a sensitive detector of mitochondrial ROS generation[72]. The following protocol describes the general procedure that was followed to stain the cells with JC-1 and Mitotracker.

1st day

- Plate 800.000 cells/ml in a 24 well plate
- Use 5μM of Nutlin-3a(10mM) for the treatment

2nd day (JC-1 staining)

1. Biological replicate harvesting

2. Firstly, Trypan-Blue assay to determine cell concentration per ml and their viability status

3. Centrifugation for 5min at 1200 rpm RT

4. Resuspension of the samples in order to obtain 400.000 cells/ml

5. Resuspension of JC-1 dye to 2ml of each sample

6. Incubation inside the incubator for 45min in a 24 well plate

7. Recollection of the samples

8. Centrifugation for 5min at 1200 rpm,RT

9. Aspirate the supernatant

10. Wash with 1xPBS

11. Centrifugation for 5min at 1200 rpm,RT

12. Aspirate the supernatant

13. Repeat 10 and 11 step twice

14. Resuspend the cells in 2ml RPMI

15. Place 100μl of each sample of each BR in a black 96-well plate

16. Before the experiment add 1μl Hoescht(1:500 dilution) in every 100μl

2nd day (Mitotracker staining)

1. Biological replicate harvesting

2. Firstly, Trypan-Blue assay to determine cell concentration per ml and their viability status (3 measurements)

3. Centrifugation for 5 min, at 1200 rpm RT

4. Place 400.000 cells/ml (the working concentration; 40000/100μl).

5. Add mitotracker RED dye (1,25 μl) to 100 μl of each sample (+/-N3a) in a black 96-well plate

6. Incubate in 370C, 5%CO2 for 15-30 min

7. Recollection of the samples (in 4 tubes—collect the technical replicates in ones)

8. Centrifuge 5 min at 1200 rpm, RT

9. Aspirate the supernatant & wash with 1xPBS (repeat steps 8-9)

10. Resuspend cells of each sample in 100 µl RPMI of each BR in the black 96-well plate

11. Before the experiment add 1µl Hoescht (1:500 dilution) in every sample (100µl)

2.13 High Content Imaging

Images are captured with a 40X lense (Olympus) with the Operetta High content screening microscope (Perkin Elmer) and analysed using Harmony software 4.1 with PhenoLOGIC (PerkinElmer).

For the analysis, nuclei are identified using the nuclear dye Hoechst which is cell permeable and can bind to DNA in live or fixed cells. The intensity of the Hoechst dye was used further to characterize the cells as live or dead. The channel capturing mitotracker or JC1 fluorescence (excitation/emission-580/600nm) are used to define the cytoplasm around the nucleus. The intensity (mean and Sum per cell) is measured in the area of the cytoplasm. The number of mitochondria per cell is estimated and the intensity of the fluorescent dye (mitotracker or JC1) was measured. For the JC1 stained cells the intensity at 580nm is measured as well to produce the ratio red/green intensity which indicates the mitochondria depolarization. Finally, the morphological characteristics of the individual mitochondria such as area, length and width are estimated.

To estimate the necrosis and apoptosis, cells are imaged with the Digital Phase Contrast channel and within the area of every cell the intensity at 580nm for Annexin V and the intensity at 650nm for Propidium iodide are measured. If the mean intensity of every cell is found above the threshold the cells are characterized apoptotic, dead or live. The threshold is estimated by measuring unstained cells or cells with a single fluorophore.

2.14 TEM (Transmission Electron Microscope) imaging of the biological samples

TEM operates on the same basic principles as the light microscope but uses electrons instead of light. The wavelength of electrons is much smaller than that of light and as a result the optimal resolution attainable for TEM images is many orders of magnitude better than that from a light microscope. Thus, TEMs can reveal the finest details of internal structure[73].TEM is the gold standard method for studying autophagy by detecting autophagosomes[74].

Cells in two conditions (before and after Nutlin-3a; 0-5µM) were fixed in 2.5% glutaraldehyde for 24 h at 4°C, washed in 0.1 M sodium cacodylate buffer (PH=7.4), post –fixed in 2% OsO4 in 0.1 M sodium cacodylate buffer for 60 min at 4°C, dehydrated in increasing concentrations of alcohol. The samples were impregnated with prophylene oxide and embedded in epoxy resin embedding media. Then ultra-thin sections were cut with LKB ultratome V-2088 and were placed on a TEM grid, post-stained with uranyl acetate and lead citrate. Images were obtained using on a LaB6 JEOL 2100 electron microscope operating at an accelerating voltage of 80 kV.

2.15 Nanoscale liquid chromatography coupled online with MS

Identification and relative quantification of proteins was done by reversed phase nano-flow chromatography coupled with electrospray ionization system and mass spectrometer (nLC-ESI-MS / MS). The peptides were dissolved in 10µl of formic acid aqueous solution of 0.5% and separated on reverse phase column (Reprosil Pur C18 AQ, particle size= 3 micrometers, pore size= 120 Angstrom (Dr. Maisch), inner diameter= 75µm, length= 15cm). The flow of small-scale elution liquid chromatography was 300 nl/min. Peptides separated and gradually eluted in water-ACN and entered the mass spectrometer.

2.16 Meta-processing of pre-existing proteomics data

Pre-existing proteomics data were used as an input to Reactome, Gene Ontology and KEGG databases to achieve the functional analysis. Reactome is a peer-reviewed pathway database which provides bioinformatic tools for the visualization, interpretation and analysis of pathways[75].The Gene Ontology website can be used to obtain information for functional genomics through ontologies which describe biological knowledge. Molecular function, cellular component and biological

processes are the three main elements of the Gene Ontology[76].KEGG is a big database comprised of different databases with information about genome, diseases and biological pathways and is an excellent tool for bioinformatics and proteomics data analysis[77]. Heatmaps were formed using the Perseus(v.4.5.) software, which is a software used for presenting the expression levels of proteins in different conditions as parallel line charts (the different cell lines are represented in the x-axis while different expression levels exist on the y axis).[78]

3.Results

3.1.1 Effect of N3a on cell viability in HL/NHL cell lines

N3a, as it was mentioned above, has the ability to activate and stabilize p53 resulting into cell cycle arrest and apoptosis. MDA-V(HL), JMP1(MCL) and SUPM2(ALCL) cell lines were treated with 5μMand 10μMof N3a for 24 hours, in order to study N3a's biological effect.

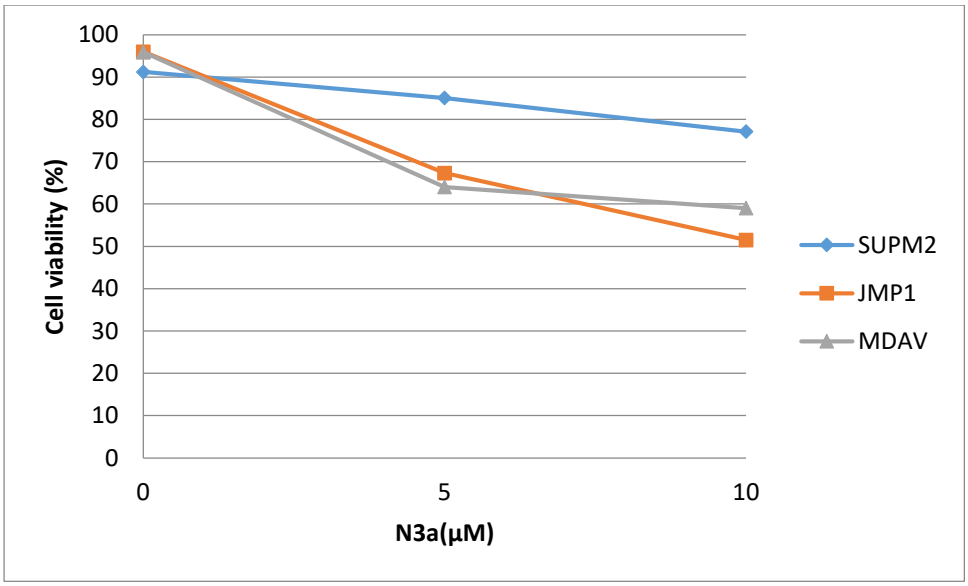

Figure 3.1. Assessment of viability after treatment with N3a in HL/NHL lymphoma cell lines using the Trypan Blue method. Decrease of cell viability was observed in all cell lines.

It was observed that N3a did block the growth and proliferation of cells. More specifically, in MDAV (HL) and JMP1 (MCL) the viability decreased from approximately 95% to 50% in 24 hours. In SUPM2, which is the cell line that corresponds to ALCL, the viability showed slight decrease (90%to 71%) in comparison to the previous cell lines.

3.1.2 Effect of N3a on cell apoptosis in HL/NHL cell lines

The estimation of cell apoptosis after treatment with 5μM N3a was performed using Annexin V and High Content Imaging, as it is described above in the section 2.13 of Materials and Methods.

Annexin V (AV) has the ability to bind to phosphatidylserine, a marker of apoptosis when it is on the outer leaflet of the plasma membrane. Along with Annexin V, Propidium Iodide (PI) was used to distinguish dead from live cells, as PI cannot cross the membrane of the living cells.

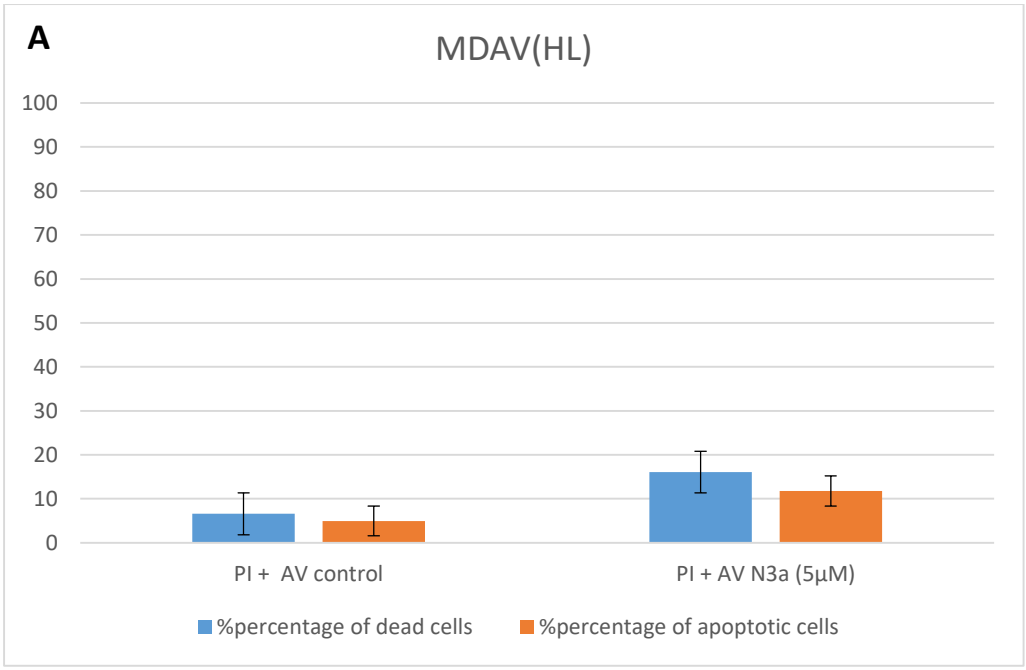
A
MDAV(HL)
100
90
80
70
60
50
40
30
20
10
0
PI + AV control
PI + AV N3a (5µM)
%percentage of dead cells
%percentage of apoptotic cells

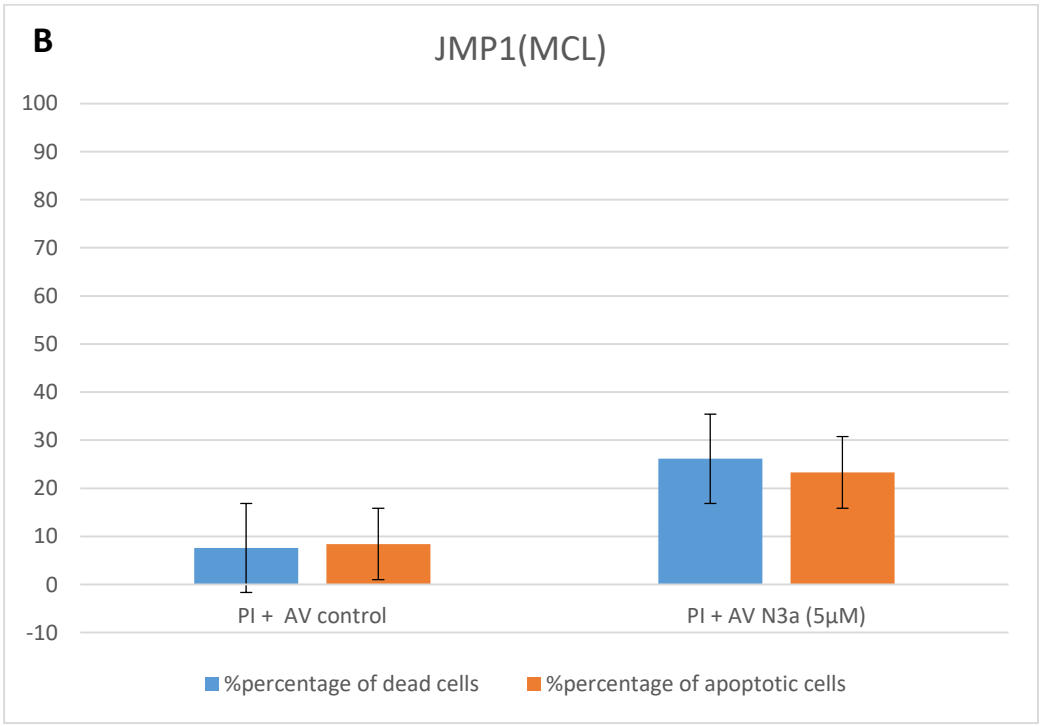
B
JMP1(MCL)
100
90
80
70
60
50
40
30
20
10
0
-10
PI + AV control
PI + AV N3a (5µM)
%percentage of dead cells
%percentage of apoptotic cells

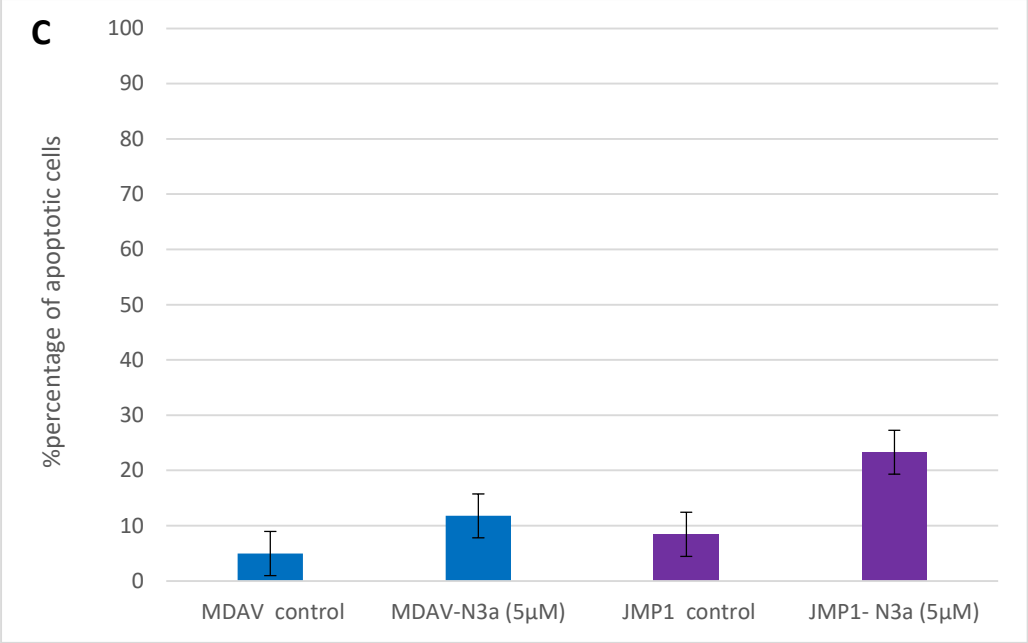

Figure 3.2. Effect of N3a on the apoptosis in JMP1 (NHL) and MDAV (HL). Treatment with 5μM N3a in HL(A) and NHL(B) cells with wt p53 led to apoptosis and comparison of the percentage of apoptotic cells in two lymphoma types (C).

The results showed an increase of apoptosis after treatment with N3a. MCL (Fig.2B) apoptosis showed higher rate than in HL (Fig.2A). In MCL apoptosis increased by 15%, whereas in HL by 7%. The difference in the percentage of apoptotic cells between the two cell lines is depicted in Fig 2(C).

3.1.3 Effect of N3a on mitochondria' depolarization

Mitochondria play a key role in apoptosis and as it was mentioned at the introduction, a fraction of p53 protein localizes to mitochondria whenp53-dependent apoptosis begins. The accumulation of p53 leads to changes in mitochondrial membrane potential and release of cytochrome c[79].

HL cell line (MDAV) and MCL (JMP1) cell line were treated with 5Mμ in a timeframe of 24 hours and then stained with the JC-1 dye and Mitotracker RedCM-H2Xros in separate experiments. The samples were observed through High Content Imaging and the results were obtained as it is described in the section 2.13 of Materials and Methods.

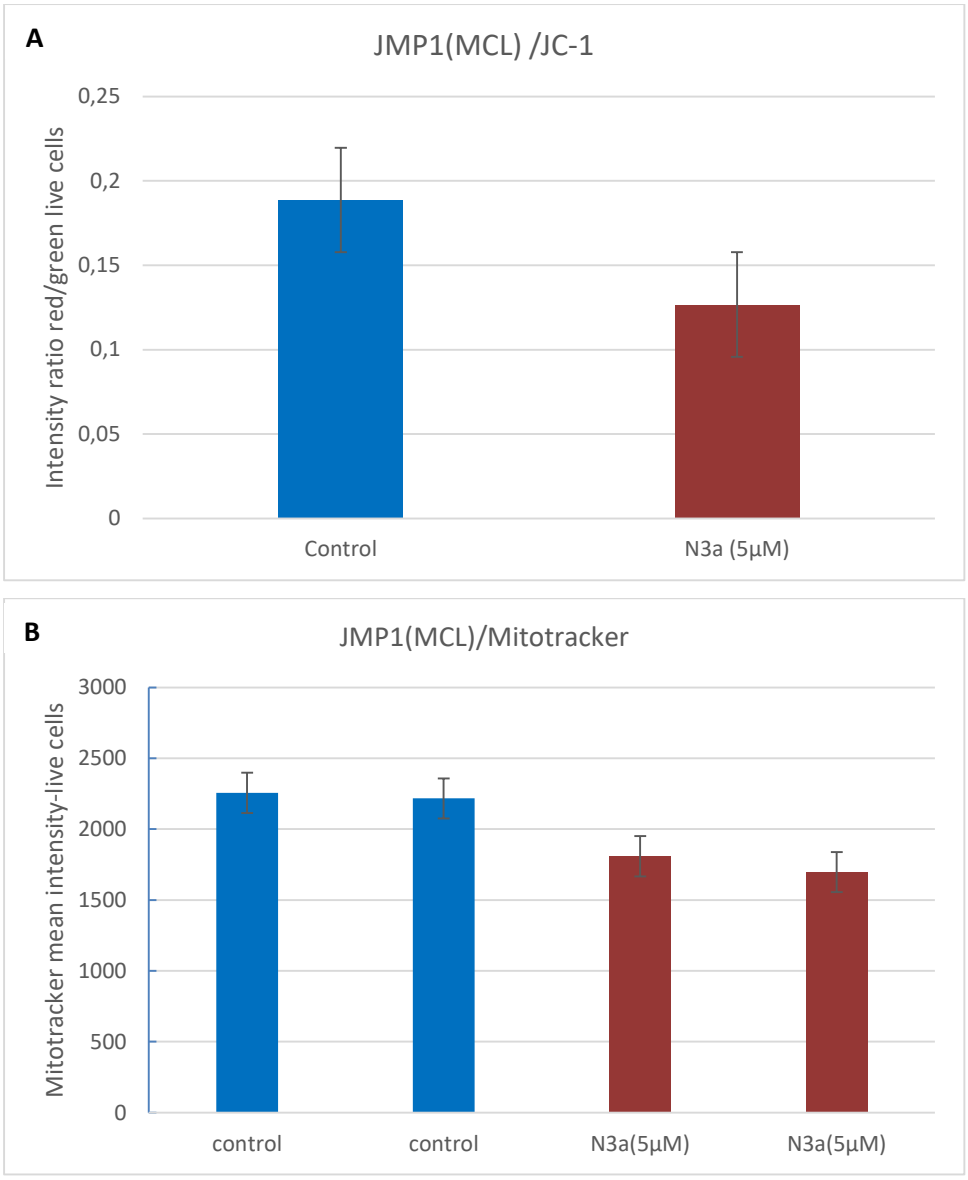

Figure 3.3. Assessment of N3a's effect on mitochondria depolarization in JMP1(MCL) using JC1 dye (A) and Mitotracker RedCM-H2Xros dye (B).

The decrease of the intensity ratio red/green after treatment with 5µM N3a on JMP1, indicates the depolarization of the membrane and thus, the apoptotic pathway is activated. When JMP1 cells are dyed with Mitotracker Red-H2Xros, the treated cells showed a decrease in the mean intensity in live cells. This decrease agrees with the results of JC-1 staining indicating depolarization of the mitochondrial membrane.

JC-1 was also used on MDAV cell line but due to technical problems through the analysis, the ratio could not be measured but instead the mean intensity in live cells was used. Mitotracker was also used to stain this cell line.

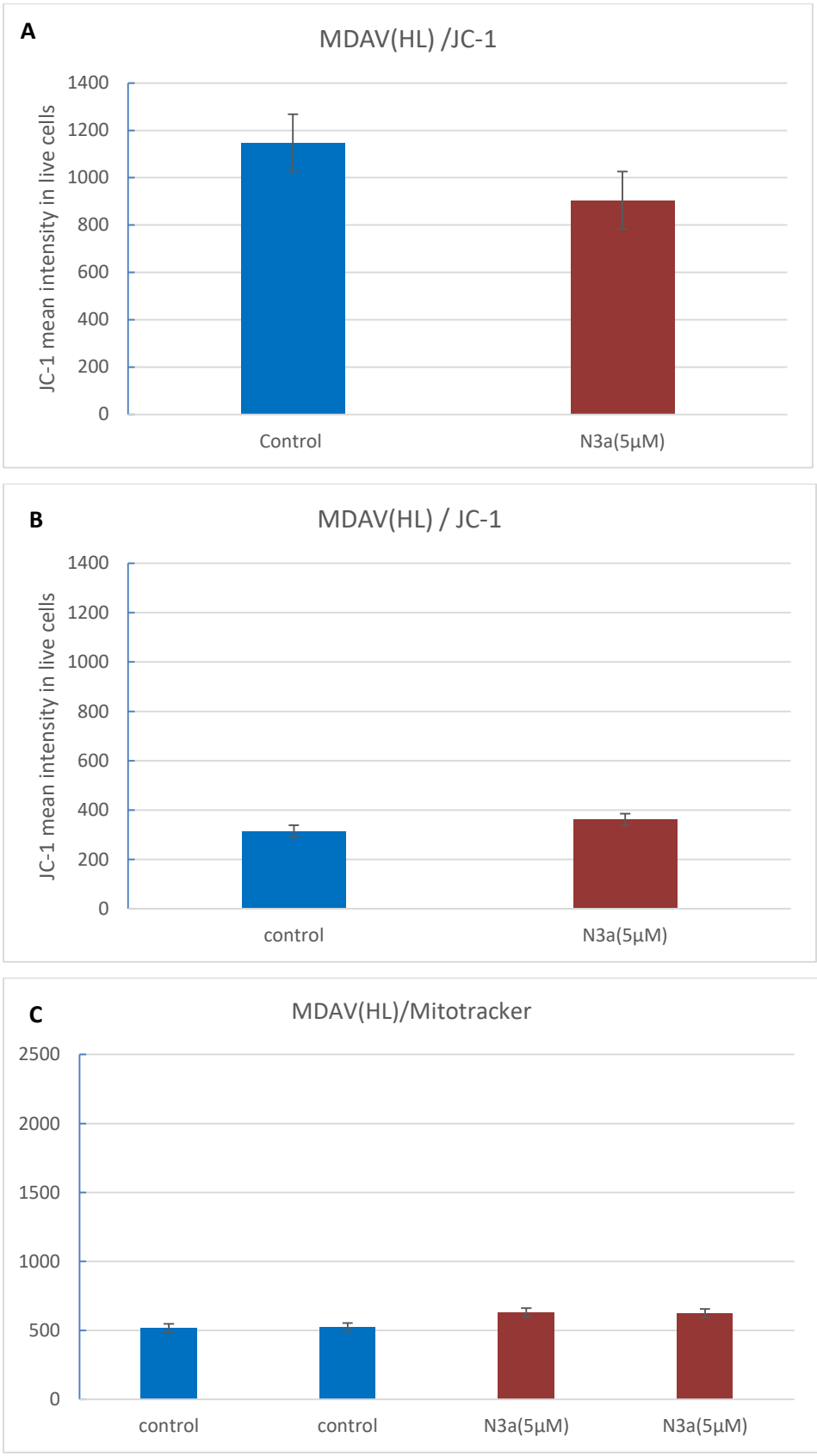

Figure 3.4. Assessment of N3a's effect on mitochondria depolarization in MDAV(HL) using JC1 dye (A), (B) and Mitotracker RedCM-H2Xros dye (C).

As it can be observed in Fig.4B, JC-1 dye showed different staining pattern in two different experiments. In the first experiment, JC-1 showed reduction after treatment whereas in the second experiment it showed an increase. The Mitotracker dye intensity was elevated by over 10% after treatment. These results cannot lead to safe conclusions and repetition of these experiments in MDAV cell line (HL) is necessary.

The same experiments were performed in the ALCL cell line, SUPM2. Due to technical problems through the analysis, the ratio of red/green of JC-1 could not be obtained. As a result, the mean intensity of JC-1 was measured in live cells.

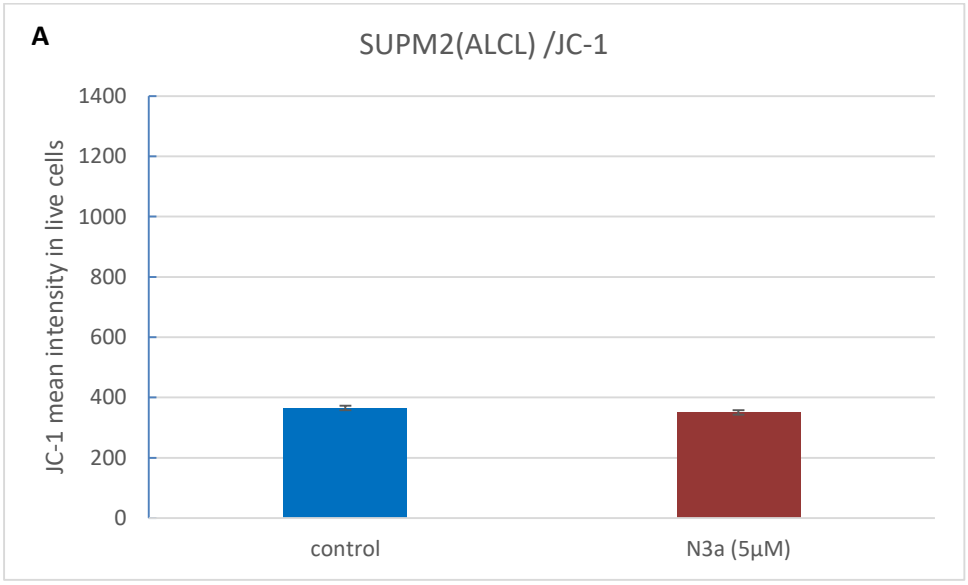

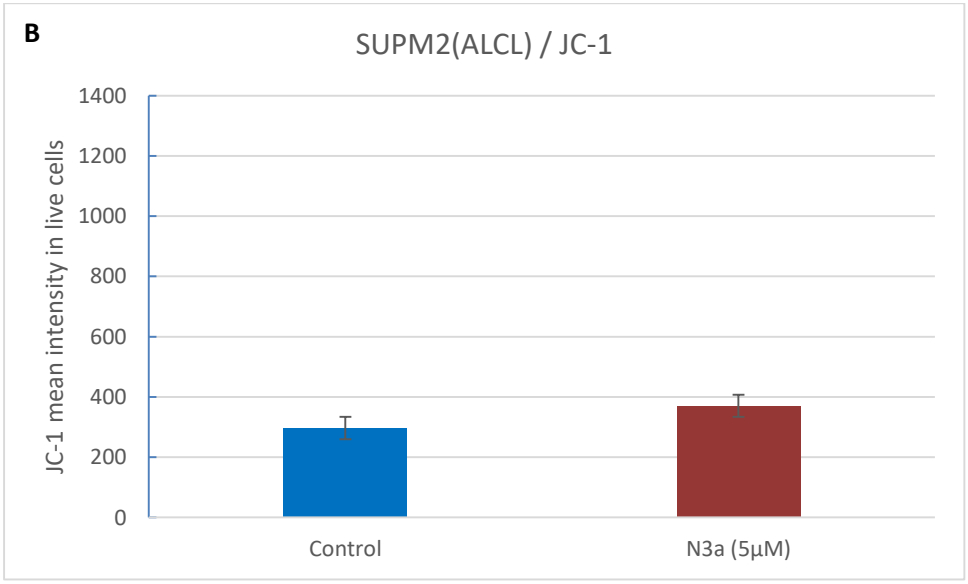

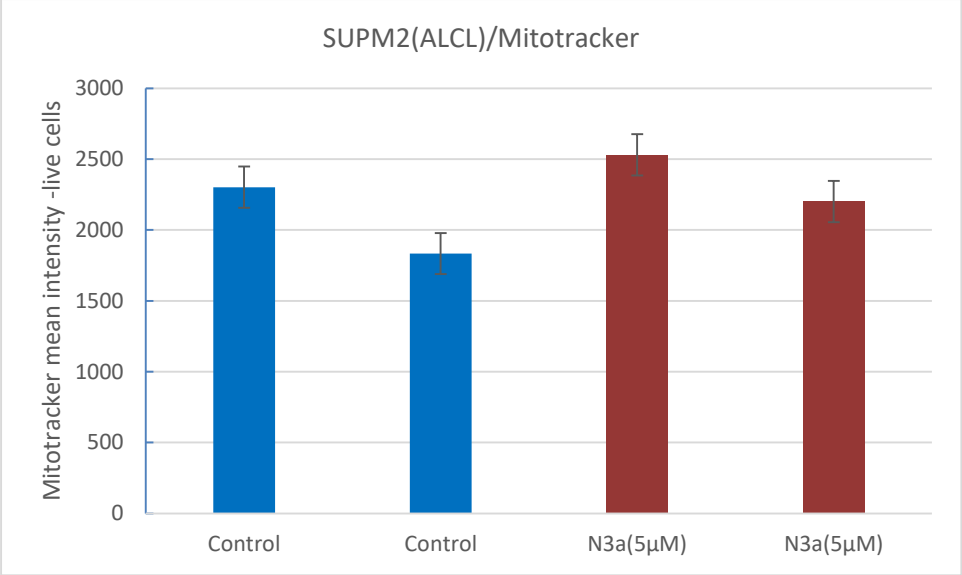

Figure 3,5. Assessment of N3a's effect on mitochondria depolarization on SUPM2(ALCL) using JC1 dye (A),(B) and Mitotracker RedCM-H2Xros dye (C).

In Fig5(A), no major changes in the intensity are observed, whereas in Fig5(B) treated cells show slightly higher intensity of JC-1. However, when cells are stained with Mitotracker RedCM-H2Xros treated cells show decreased intensity. Safe conclusions for this cell line cannot be made and repetitions of these experiments are needed.

3.2. Proteomic analysis of HL/NHL cell lines after treatment with N3a

The proteomic analysis of each lymphoma cell line after treatment with N3a, revealed a total of 4926 proteins. From these 4926 proteins, 3333 were found to be expressed in all lymphoma cell lines, whereas 420,321 and 399 proteins were expressed in HL, MCL and ALCL cell lines respectively. After treatment with N3a ,3578 out of 4926 proteins were found to be deregulated. More specifically,2246 proteins were deregulated in HL,2159 in MCL and 1489 in ALCL. Out of the 3578 proteins, 585 were expressed in all lymphoma types, whereas 732,655 and 461 proteins were expressed uniquely in HL, MCL and ALCL respectively. It is important to note that HL and MCL shared the highest number of proteins (702), while ALCL shared approximately the same amount of proteins with both HL and MCL.

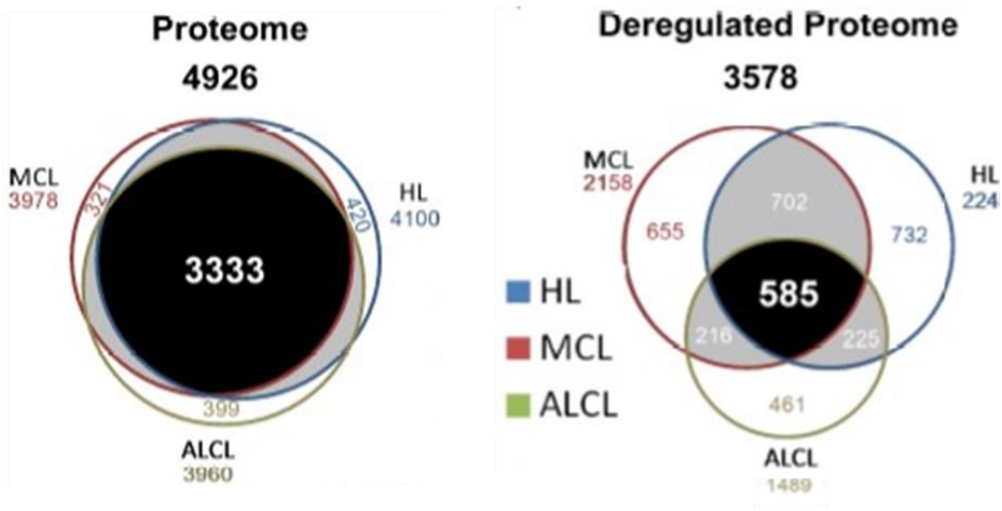

Figure 3.6. Venn diagrams showing the total and deregulated proteome in HL, MCL and ALCL after treatment with N3a.

3.2.1 Effect of N3a on autophagy

As it was mentioned above, through the proteomic analysis 4926 proteins were identified in all lymphoma cell lines. It was revealed, through pathway analysis using KEGG database, Gene Ontology and Reactome, that 163 proteins out of the 4926 were involved in the autophagy pathway. From these 163 proteins,99 were expressed in all lymphoma cell lines. It is important to highlight that again HL and MCL had the most proteins in common than HL with ALCL and MCL with ALCL.

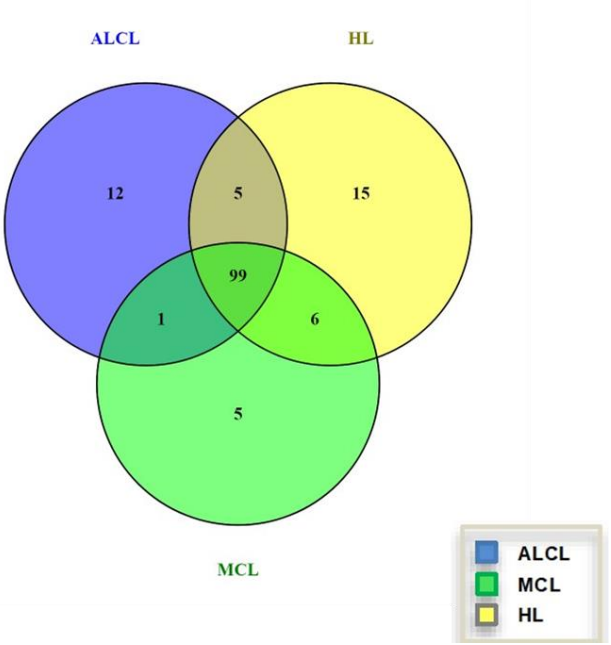

Figure 3.7. Venn diagram showing the 163 differentially expressed proteins linked to autophagy in lymphoma cell lines after treatment with N3a.

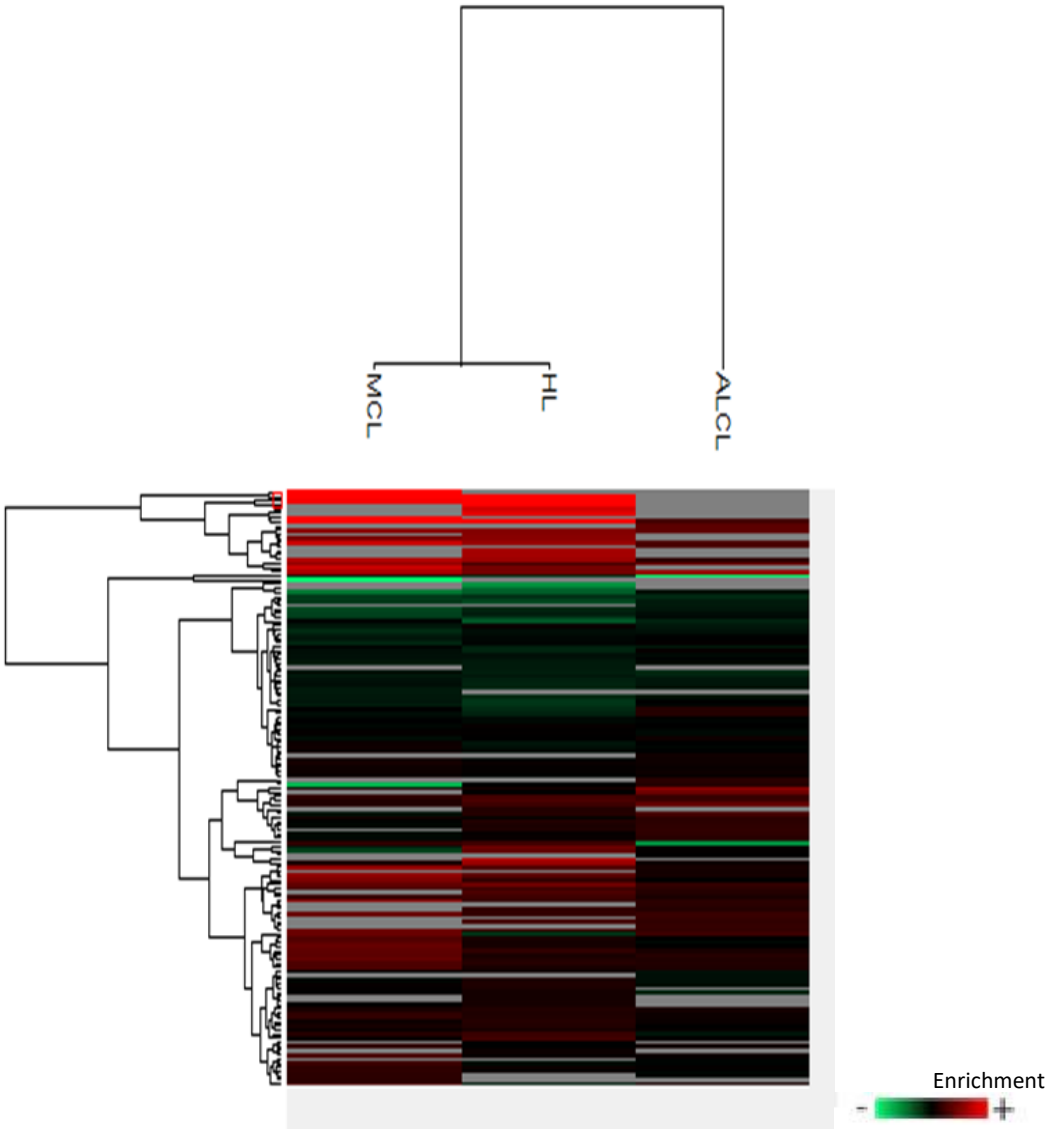

Figure 3.8. Heatmap showing the expression profile of proteins in all lymphoma cell lines after treatment with N3a. Green indicates downregulated proteins, red upregulated proteins and grey stable protein expression status.

A heatmap can be considered a table which does not use numbers but colours, in order to visualize the expression levels of proteins. The green color indicates low expression; the red color is used for high expression while black is used to indicate no changes in the expression levels. Grouping objects with similar values is obtained through clustering and each row is considered as a cluster. Hierarchical clustering starts to combine the two most similar clusters and continues to combine until all objects are in the same cluster and this eventually leads to a dendrogram. The

dendrogram depicts the hierarchy of the clusters. In our results, we performed unsupervised hierarchical clustering, where each row represents the abundance values of proteins, whereas cell lines are represented as columns. As it can be seen in Fig. 3.8, autophagy proteins after treatment with N3a tend to be upregulated, and HL with MCL were separated from ALCL in one main branch of the dendrogram.

3.3.1 Western blotting to monitor N3a's effect on autophagy

Western blotting was performed to verify the results of the proteomic analysis performed on the autophagy-related proteins. The selection of the proteins was made in accordance with their relativity to the process of autophagy. As a result, ATG5/ATG12 conjugate, ATG4B and LC3I/II were selected in order to perform western blot analysis and actin was used as a loading control.

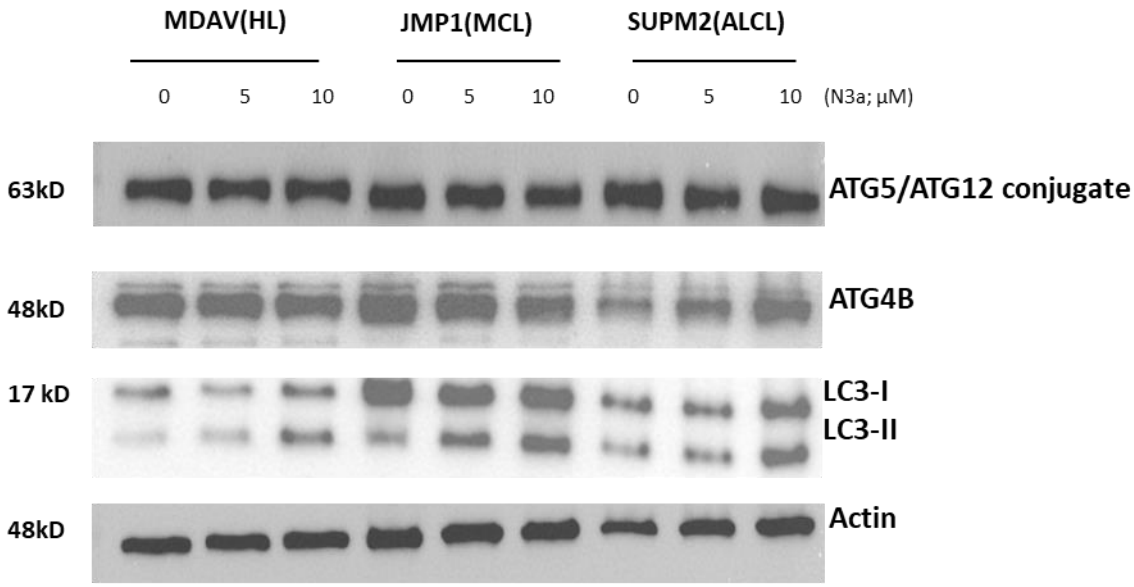

Figure 3.9. Western Blot analysis performed on HL (MDAV) and NHL (JMP-1 and SUPM2) cell lines to verify proteomic analysis on autophagy pathway. Treatment with N3a in three different concentrations suggesting activation of autophagy.

ATG4b plays a dual role for autophagy as it cleaves the pro-LC3 generating a C terminal glycine for the PE conjugation and also hydrolases LC3II at the end of autophagy. ATG4b is equally expressed in HL, while in MCL a slight decreased expression is observed at 10μM.The Atg12-Atg5 conjugate is a ubiquitin-protein ligase (E3)-like enzyme for Atg8-PE conjugation reaction. Specifically, ATG5/ATG12 activates ATG3 which covalently binds ATG8 to PE in the surface of autophagosomes and as a result

lipidated LC3 leads to the closure of the autophagosomes. ATG5/ATG12 levels appear to be the same among the two lymphoma types. The lipid modified form of LC3, referred to as LC3-II, is believed to be involved in autophagosome membrane expansion and fusion events. The LC3-II increase compared to LC3-I indicates induction of autophagy and a conclusion can be extracted when results are compared to levels of actin.LC3-I to LC3-II protein levels appear to be more elevated at 10μM in HL, whereas in MCL the expression is gradually elevated from 0 to 5μM of N3a.In SUPM2, ATG4b and LC3-I to LC3-II are more expressed at 10μM than 5μM, indicating stronger activation of autophagy at 10μM. However, results for the untreated sample and comparison between it and the treated samples cannot be made without the use of software normalization and due to the limited timeframe was not available to use.

3.3.2 Western Blotting to monitor N3a's effect on NFκBsignaling.

Western blotting was performed to assess the effect of N3a on the NFκB signaling. The selection of the proteins was made in accordance to their relativity to this signaling pathway. As a result, western blotting was performed on p65 and p-p65.Western blotting was also performed on IKKβ and IKβ but due to technical difficulties a result could not be obtained.

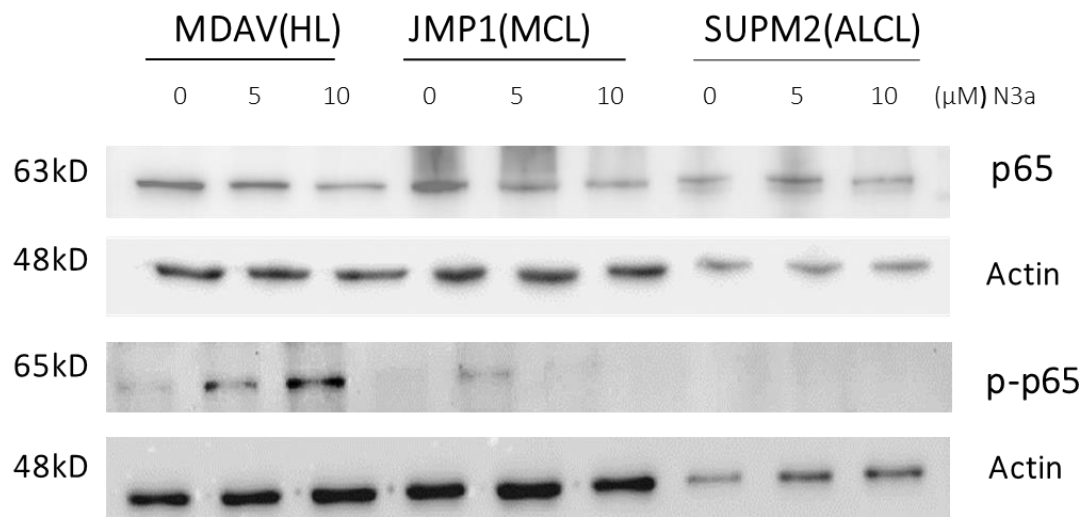

Figure 3.10. Western Blotting to monitor the NFκB signaling after treatment with 5μM N3a

In HL and MCL p65 is more expressed at 0 and 5μM, whereas in ALCL it is equally expressed among 0-10mM concentrations. p-p65 is more expressed in MDAV at

10μMand by comparing it to its unphosphorylated form, it can be concluded that NFκB might be activated. p-p65 does not show in other cell lines, but repetition of this experiment is advised to exclude technical errors before making any further conclusions.

3.4 Ultrastructural analysis by Transmission Electron Microscopy (TEM) in lymphoma cells, before and after treatment with N3a.

The MDA-V cell line, which corresponds to Hodgkin lymphoma, was treated with 5μM N3a for 24 hours. After 24 hours, cells were collected and prepared for TEM imaging as it is described in section 2.14 of Materials and Methods. The purpose for this experiment was to obtain images, focusing on lymphoma cells after treatment. Many images were obtained with the microscope but the most representative ones will be shown in this thesis.

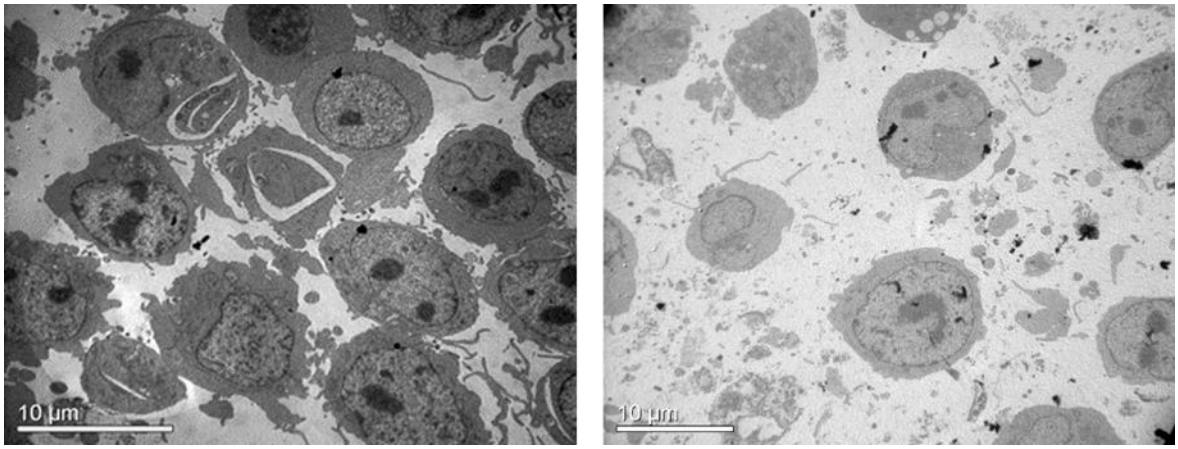

Figure 3.11. Ultrastructural analysis by TEM before and after treatment with N3a. The left image corresponds to non-treated lymphoma cells, whereas the right image depicts treated lymphoma cells with 5μM N3a. The magnifications is x10.

As it can be observed in figure 3.11, the population of the non-treated cells is greater than the one of the treated cells. It can also be observed that many cell fragments exist between the cells.

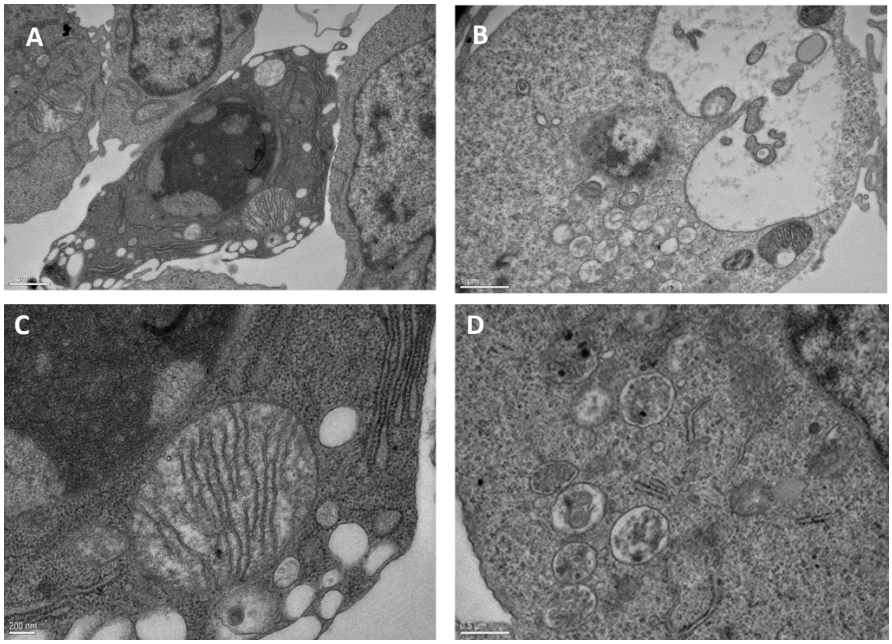

Figure 3.12. Low and high magnification images of non-treated lymphoma cells imaged by TEM. Top pictures have a scale of 1µm, the bottom left 200nm and the bottom right 0,5µm.

Many empty vacuoles are observed in untreated cells in Fig.3.12, but also vacuoles that contain material. The latter vacuoles may have material for degradation or exportation or maybe material imported to the cell prior taking this image. The mitochondria appear swollen and cell fragmentation is also observed. Finally, chromatin clumping inside the nucleus is observed.

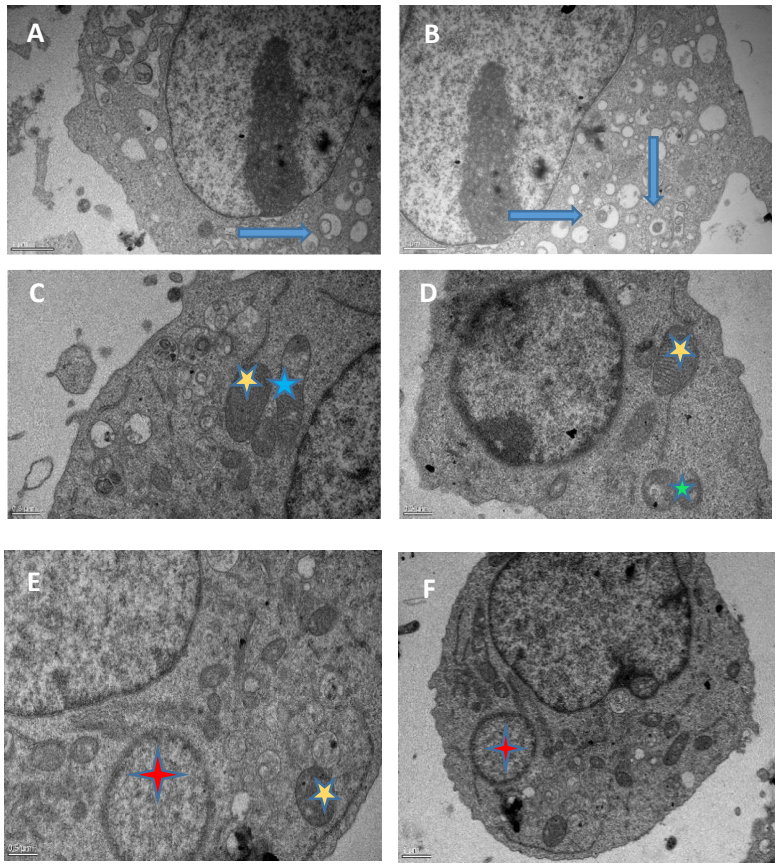

Figure 3.13. Low and high magnification images of Treated lymphoma cells with 5µM N3a imaged by TEM. Top pictures have a scale of 1µm and the bottom ones have 0,5µm.

After treatment with 5µM of N3a, the cells obtain the morphology pictured in Fig.13. There is chromatin clumping inside the nucleus and also nuclear fragmentation, indicated by the red star in pictures (E) and (F). Potential autophagosomes are observed in pictures 3.13 (A) and (B) and are indicated by the blue arrows. The mitochondria, depicted by the yellow star, appear swollen and some elongated (blue star), possibly corresponding to mitochondrial fusion. In picture3.13(D), the structure indicated by the green star might be fission of the mitochondria. In addition, in pictures 3.13 (C), (D), (E) and (F) there are possibly smaller-sized mitochondria, which could be product of mitochondrial fission.

4.Discussion

The heterogeneity of lymphomas is the major issue that leads to different responses to treatments. Despite the fact that the survival rate has increased in the last decades, many patients and particularly elderly people, do not respond to treatments and in fact, the chemotherapy regimens used are not well-tolerated by them[40]. Thus, it is of great need to find new ways for developing new, more tolerable and more efficient treatments. Molecular targeted therapies are emerging and the autophagic signaling pathway is of great interest. Autophagy is a signaling pathway that has been shown to interact with the procedure of apoptosis, in a direct or indirect manner[80]. In addition, autophagy does not have a clear role in the initiation and progression of lymphoma and its effect on therapeutic interventions is multi-faced[40]. The NF-κB signaling pathway and its aberrant deregulated activation is also a hallmark of many lymphoid malignancies[51,81], and as a result it is of great interest. Nutlin-3a (N3a) is a cis-imidazole compound that displaces p53 from MDM-2 and stabilizes but also activates the p53 pathway[34] and leads to apoptosis. This non-genotoxic activation of p53 by N3a and its effect on autophagy and the NFκB signaling pathway have not been studied before in lymphoma. Thus, it seemed interesting to assess N3a's effect on these signaling pathways.

Cells from three lymphoma types when treated with two different concentrations of N3a (5μM, 10μM) showed decreased cell viability, with ALCL showing the lowest. Annexin V staining of the cells after treatment with N3a also revealed that HL and MCL were successfully driven to apoptosis, a fact that confirms the effect of N3a. In addition to Annexin, experiments with mitochondrial dyes such as JC-1 and Mitotracker RedCM-H2Xros were performed using High Content Imaging. After staining with dye JC-1 ,the intensity of red/green ratio in MCL showed a decrease, which agrees with the mitochondrial membrane potential collapse during the process of apoptosis[82].The Mitotracker RedCM-H2Xros staining revealed a similar pattern with JC-1 dye and possibly indicates the mitochondrial membrane depolarization HL the results were controversial, as one experiment showed an increase in red intensity, whereas the other one depicted a decrease in the intensity. The Mitotracker RedCM-

H2Xros staining in HL showed an increase after treatment which contradicts the results by JC-1 dye. It should be taken under consideration that Mitotracker RedCM-H2Xros is a dye sensitive for ROS generation[72] and production of ROS is observed in early stages of programmed cell death[83]. Therefore, the increase of Mitotracker RedCM-H2Xros might be attributed to the production of ROS, which occurs in the early stages of programmed cell death induced by N3a. In ALCL, in the first biological replicate, the JC-1 red intensity was the same in untreated and treated lymphoma cells, while the second biological replicate showed an increase after treatment. The Mitotracker RedCM-H2Xros staining in ALCL showed similar pattern with the HL staining. The results obtained from these experiments cannot lead to safe conclusions and further experiments are suggested.

After profiling the global proteome of HL/MCL/ALCL before and after treatment with N3a, out of the 3578 deregulated proteins, 585 were expressed in all lymphoma types, whereas 732, 655 and 461 proteins were expressed uniquely in HL, MCL and ALCL, respectively. It is important to note that HL and MCL shared the highest number of proteins (702) when ALCL shared the same amount of proteins with both HL and MCL(Fig.6). The similarity between the protein signature after treatment with N3a in HL and MCL might be due to the fact that both cell lines used to represent these lymphoma types, are B cells. Using the data from the proteomic analysis and focusing only on proteins involved in the autophagic pathway, it was noticed that after treatment with N3a the heatmap (Fig.8) showed an enrichment in protein expression levels. Again, HL and MCL had similar protein expression status and as it was mentioned above, this is due to the fact that both cell lines originate from B cells. In order to verify the proteomics analysis results, Western Blot was performed to study the effect of N3a on the autophagic pathway. Our preliminary results suggest that the autophagy pathway is activated in HL and MCL after treatment. Indeed, Pujals et al. working on Burkitt lymphoma have shown that treatment with N3a on EBV (Epstein Barr Virus) positive B cells tend to upregulate expression of autophagy-related proteins, which will contribute to drug resistance[84]. The two EBV positive of our cell lines are indeed HL, MCL and when treated with various concentrations of N3a, the autophagy related proteins were found to be upregulated. Monette et al. support that

wtTP53 induces autophagy, which promotes the survival of the lymphoma cells by recycling toxic intracellular material and inhibiting apoptosis[80]. Given the fact that N3a has the ability to displace MDM2 and reactivate the wt-p53, treatment with N3a might lead to upregulation of autophagy. Drakos et al. have indeed verified the apoptotic effect of N3a in MCL cells, demonstrating also that N3a downregulates the mTOR pathway, which inhibits autophagy and as a result, possible activation of the autophagic pathway might be detected[85]. It should be highlighted that the results from the Western Blot are only indicative, and they must be performed again to ensure that autophagy is truly upregulated.

Transmission Electron Microscope (TEM) is the golden standard method to study autophagy[74] and as a result, the decision was made to originally check our Hodgkin lymphoma cell line before and after treatment with N3a (5μM) and study its effect. Before the treatment, cells showed a structure which resembles apoptotic phenotype with condensed chromatin, cell fragmentation and swollen mitochondria. After the treatment, these characteristics were more defined and possible autophagosomes were detected, as double membrane vacuoles were observed. In addition, mitochondria of smaller size were detected, which possibly correspond to mitochondria undergoing fission, as part of the programmed cell death after activation of p53. Karbowski et al. have previously demonstrated that when programmed cell death is activated, it leads to mitochondria fission[86]. Mitochondria fission also happens when autophagy is activated to remove damaged mitochondria with a process called mitophagy[87]. Although enclosed mitochondria to autophagosomes were not observed, the smaller sized mitochondria could be led to mitophagy in a later stage. Finally, an effort was made to study the effect of N3a on NF-κB signaling pathway as it is deregulated in HL[88] and many B and T cell lymphomas[50]. Due to technical difficulties, mainly concerning low sensitivity of antibodies (either due to low epitope abundance, or poor antibody affinity) and limited experiment-timeframe, only p65 and p-p65 were successfully studied using Western Blot. The phosphorylated form of p65 showed increase after treatment with N3a only in Hodgkin lymphoma cells, as signal from the other cell lines was not detected. It should be highlighted that that induction of p53 causes an activation of

NF-kB that correlates with the ability of p53 to induce apoptosis[89]. However, conclusion for the NF-κB signaling cannot be safely made using only these experiments, and repetition of immunoblots using also other antibodies, such as of Ikβα must be performed. This is mentioned, since in MCL, previous study has shown that there is a constitutive activation of the NF-κB signaling[90], but in our results MCL cells did not show any expression of p-p65. This fact, along with the failed sensitivity of antibodies may agree with technical errors. To better study the NF-κB signaling, cell fractionation to obtain cytosolic and nuclear fragments are recommended to be performed. Western Blotting for p65 is also suggested, in order to detect its translocation to the nucleus using the fractionated lysates.

To conclude, our results verified the apoptotic effect of N3a in the three lymphoma types of our study: HL, MCL and ALCL and also indicated a deregulation of the mitochondria's membrane potential. They also indicated an increase in the autophagic pathway after treatment with different concentrations of the cis-imidazole compound, N3a. However, further *in vitro* and *in vivo* experiments must be performed to assess the effect of N3a on the autophagy pathway and to explore whether its activation may contribute to drug resistance.

5.References

1. PDQ Adult Treatment Editorial Board. *Adult Hodgkin Lymphoma Treatment (PDQ®): Patient Version*. *PDQ Cancer Information Summaries* (2002).

2. Vardhana, S. & Younes, A. The immune microenvironment in hodgkin lymphoma: T cells, B cells, and immune checkpoints. *Haematologica* **101,** 794–802 (2016).

3. Smedby, K. E., Baecklund, E. & Askling, J. Malignant lymphomas in autoimmunity and inflammation: A review of risks, risk factors, and lymphoma characteristics. *Cancer Epidemiol. Biomarkers Prev.* **15,** 2069–2077 (2006).

4. Filipovich, A. H., Mathur, A., Kamat, D. & Shapiro, R. S. Primary immunodeficiencies: genetic risk factors for lymphoma. *Cancer Res.* **52,** 5465s–5467s (1992).

5. Maeda, E. *et al.* Spectrum of Epstein-Barr virus-related diseases: a pictorial review. *Jpn. J. Radiol.* **27,** 4–19 (2009).

6. Grulich, A. E. *et al.* B-cell stimulation and prolonged immune deficiency are risk factors for non-Hodgkin{\textquotesingle}s lymphoma in people with {AIDS}. *Aids* **14,** 133–140 (2000).

7. Lymphoma - Symptoms and causes - Mayo Clinic. Available at: https://www.mayoclinic.org/diseases-conditions/lymphoma/symptoms-causes/syc-20352638. (Accessed: 26th August 2018)

8. King, R. L., Howard, M. T. & Bagg, A. Hodgkin Lymphoma. *Adv. Anat. Pathol.* **21,** 17–30 (2014).

9. Cantor, K. P. *et al.* Pesticides and other agricultural risk factors for non-Hodgkin's lymphoma among men in Iowa and Minnesota. *Cancer Res.* **52,** 2447–55 (1992).

10. Lymphoma - Diagnosis and treatment - Mayo Clinic. Available at: https://www.mayoclinic.org/diseases-conditions/lymphoma/diagnosis-

treatment/drc-20352642. (Accessed: 26th August 2018)

11. Carbone, P. P., Kaplan, H. S., Musshoff, K., Smithers, D. W. & Tubiana, M. Report of the Committee on Hodgkin's Disease Staging Classification. *Cancer Res.* **31,** 1860–1 (1971).

12. Drakos, E. *et al.* Nodular lymphocyte predominant hodgkin lymphoma with clusters of lp cells, acute inflammation, and fibrosis: A syncytial variant. *Am. J. Surg. Pathol.* **33,** 1725–1731 (2009).

13. Vogt, N., Dai, B., Erdmann, T., Berdel, W. E. & Lenz, G. The molecular pathogenesis of mantle cell lymphoma. *Leuk. Lymphoma* **58,** 1530–1537 (2017).

14. Cortelazzo, S., Ponzoni, M., Ferreri, A. J. M. & Dreyling, M. Mantle cell lymphoma. *Crit. Rev. Oncol. Hematol.* **82,** 78–101 (2012).

15. Chan, J. A., Bu, X., Lai, K. K. & Nathwani, B. N. Mantle Cell Lymphoma, "Blastoid" Variant (WHO Classification), Producing Distinctive Morphologic Patterns. *Pathol. Case Rev.* **7,** 88–96 (2002).

16. Rapkiewicz, A., Wen, H., Sen, F. & Das, K. Cytomorphologic examination of anaplastic large cell lymphoma by fine-needle aspiration cytology. *Cancer* **111,** 499–507 (2007).

17. Eyre, T. A., Khan, D., Hall, G. W. & Collins, G. P. Anaplastic lymphoma kinase-positive anaplastic large cell lymphoma: Current and future perspectives in adult and paediatric disease. *Eur. J. Haematol.* **93,** 455–468 (2014).

18. Morris, S. *et al.* Fusion of a kinase gene, ALK, to a nucleolar protein gene, NPM, in non-Hodgkin's lymphoma. *Science (80-.).* **263,** 1281–1284 (1994).

19. Chiarle, R., Voena, C., Ambrogio, C., Piva, R. & Inghirami, G. The anaplastic lymphoma kinase in the pathogenesis of cancer. *Nat. Rev. Cancer* **8,** 11–23 (2008).

20. Ventura, R. A. *et al.* Centrosome abnormalities in ALK-positive anaplastic large-cell lymphoma. *Leukemia* **18,** 1910–1911 (2004).

21. Hsu, F. Y.-Y., Johnston, P. B., Burke, K. A. & Zhao, Y. The Expression of CD30 in Anaplastic Large Cell Lymphoma Is Regulated by Nucleophosmin-Anaplastic Lymphoma Kinase–Mediated JunB Level in a Cell Type–Specific Manner. *Cancer Res.* **66,** 9002–9008 (2006).

22. Rassidakis, G. Z. & Drakos, E. The emerging role of CD30 and p53 as novel targets for therapy in anaplastic large cell lymphoma. *Front. Biosci. (Scholar Ed.* 61–71 (2015).

23. Pletneva, M. A. & Smith, L. B. Anaplastic Large Cell Lymphoma Features Presenting Diagnostic Challenges. *Arch Pathol Lab Med* **138,** 1290–1294 (2014).

24. Vogelstein, B., Lane, D. & Levine, A. J. Surfing the p53 network. *Nature* **408,** 307–310 (2000).

25. Schuler, M. & Green, D. R. Transcription, apoptosis and p53: catch-22. *Trends Genet.* **21,** 182–7 (2005).

26. Steele, A. J. *et al.* p53-mediated apoptosis of CLL cells: evidence for a transcription-independent mechanism. *Blood* **112,** 3827–3834 (2008).

27. Toledo, F. & Wahl, G. M. MDM2 and MDM4: p53 regulators as targets in anticancer therapy. *Int. J. Biochem. Cell Biol.* **39,** 1476–1482 (2007).

28. Brooks, C. L. & Gu, W. p53 Ubiquitination: Mdm2 and Beyond. *Mol. Cell* **21,** 307–315 (2006).

29. Wang, W. & El-Deiry, W. S. Restoration of p53 to limit tumor growth. *Curr. Opin. Oncol.* **20,** 90–96 (2008).

30. Bond, G. L., Hu, W. & Levine, A. J. MDM2 is a central node in the p53 pathway: 12 years and counting. *Curr. Cancer Drug Targets* **5,** 3–8 (2005).

31. Vassilev, L. T. *et al.* In Vivo Activation of the p53 Pathway by Small-Molecule Antagonists of MDM2. *Science (80-.).* **303,** 844–848 (2004).

32. Patton, J. T. *et al.* Levels of HdmX Expression Dictate the Sensitivity of Normal and Transformed Cells to Nutlin-3. *Cancer Res.* **66,** 3169–3176 (2006).

33. Xia, M. *et al.* Elevated MDM2 boosts the apoptotic activity of p53-MDM2 binding inhibitors by facilitating MDMX degradation. *Cell Cycle* **7,** 1604–1612 (2008).

34. Secchiero, P., Bosco, R., Celeghini, C. & Zauli, G. Recent Advances in the Therapeutic Perspectives of Nutlin-3 MDM2. 569–577 (2011).

35. Mitani, N., Niwa, Y. & Okamoto, Y. *Surveyor TM nuclease-based detection of p53 gene mutations in haematological malignancy*.

36. Newcomb, E. W. P53 Gene Mutations in Lymphoid Diseases and Their Possible Relevance to Drug Resistance. *Leuk. Lymphoma* **17,** 211–221 (1995).

37. Antagonist in Leukemia. **22,** 868–876 (2016).

38. Wullschleger, S., Loewith, R. & Hall, M. N. TOR Signaling in Growth and Metabolism. *Cell* **124,** 471–484 (2006).

39. Kroemer, G., Mariño, G. & Levine, B. Autophagy and the Integrated Stress Response. *Mol. Cell* **40,** 280–293 (2010).

40. Pierdominici, M. *et al.* Autophagy as a pathogenic mechanism and drug target in lymphoproliferative disorders. doi:10.1096/fj.13-235655

41. Tasdemir, E. *et al.* A dual role of p53 in the control of autophagy. *Autophagy* **4,** 810–4 (2008).

42. White, E. Deconvoluting the context-dependent role for autophagy in cancer. *Nat. Rev. Cancer* **12,** 401–410 (2012).

43. Sosa, M. S., Bragado, P., Debnath, J. & Aguirre-Ghiso, J. A. Regulation of Tumor Cell Dormancy by Tissue Microenvironments and Autophagy. in *Advances in experimental medicine and biology* **734,** 73–89 (2013).

44. Qu, X. *et al.* Promotion of tumorigenesis by heterozygous disruption of the beclin 1 autophagy gene. *J. Clin. Invest.* **112,** 1809–1820 (2003).

45. Pyo, J.-O. *et al.* Essential Roles of Atg5 and FADD in Autophagic Cell Death. *J. Biol. Chem.* **280,** 20722–20729 (2005).

46. Iqbal, J. *et al.* Genomic analyses reveal global functional alterations that promote tumor growth and novel tumor suppressor genes in natural killer-cell malignancies. *Leukemia* **23,** 1139–1151 (2009).

47. Han, J. *et al.* Involvement of Protective Autophagy in TRAIL Resistance of Apoptosis-defective Tumor Cells. *J. Biol. Chem.* **283,** 19665–19677 (2008).

48. Hayden, M. S. & Ghosh, S. Signaling to NF- B. *Genes Dev.* **18,** 2195–2224 (2004).

49. Bonizzi, G. & Karin, M. The two NF-κB activation pathways and their role in innate and adaptive immunity. *Trends Immunol.* **25,** 280–288 (2004).

50. Jost, P. J. & Ruland, J. Review in translational hematology Aberrant NF- B signaling in lymphoma : mechanisms , consequences , and therapeutic implications. *Blood* **109,** 2700–2708 (2015).

51. Gasparini, C., Celeghini, C., Monasta, L. & Zauli, G. NF-κB pathways in hematological malignancies. *Cell. Mol. Life Sci.* **71,** 2083–2102 (2014).

52. Derudder, E. *et al.* RelB/p50 Dimers Are Differentially Regulated by Tumor Necrosis Factor-α and Lymphotoxin-β Receptor Activation. *J. Biol. Chem.* **278,** 23278–23284 (2003).

53. Bargou, R. C. *et al.* High-level nuclear NF-kappa B and Oct-2 is a common feature of cultured Hodgkin/Reed-Sternberg cells. *Blood* **87,** 4340–7 (1996).

54. Cabannes, E., Khan, G., Aillet, F., Jarrett, R. F. & Hay, R. T. Mutations in the IkBa gene in Hodgkin's disease suggest a tumour suppressor role for IκBα. *Oncogene* **18,** 3063–3070 (1999).

55. Jungnickel, B. *et al.* Clonal deleterious mutations in the IkappaBalpha gene in the malignant cells in Hodgkin's lymphoma. *J. Exp. Med.* **191,** 395–402 (2000).

56. Stein, H. *et al.* Identification of Hodgkin and sternberg-reed cells as a unique cell type derived from a newly-detected small-cell population. *Int. J. Cancer* **30,** 445–459 (1982).

57. Gruss, H. J. *et al.* Expression and function of CD40 on Hodgkin and Reed-

Sternberg cells and the possible relevance for Hodgkin's disease. *Blood* **84,** 2305–14 (1994).

58. Fiumara, P. *et al.* Functional expression of receptor activator of nuclear factor kappaB in Hodgkin disease cell lines. *Blood* **98,** 2784–90 (2001).

59. Deacon, E. M. *et al.* Epstein-Barr virus and Hodgkin's disease: transcriptional analysis of virus latency in the malignant cells. *J. Exp. Med.* **177,** 339–49 (1993).

60. Lake, A. *et al.* Mutations of *NFKBIA* , encoding IκBα, are a recurrent finding in classical Hodgkin lymphoma but are not a unifying feature of non-EBV-associated cases. *Int. J. Cancer* **125,** 1334–1342 (2009).

61. Psatha, K. *et al.* Deciphering lymphoma pathogenesis via state-of-the-art mass spectrometry-based quantitative proteomics. *J. Chromatogr. B Anal. Technol. Biomed. Life Sci.* **1047,** 2–14 (2017).

62. Ανατομικής, Α. Ε. Π., Πατσούρης, Δ. Κ. Ε. & Ψαθά, Κ. Α. Κλινικοεργαστηριακός Τομέας " Γενωμική και πρωτεωμική ανάλυση της επαγωγής του ογκοκατασταλτικού γονιδίου γονιδίο p53 σε Hodgkin και μη-Hodgkin μη λεμφώματα ". (2015).

63. Goy, A. *et al.* Establishment and characterization of a new mantle cell lymphoma cell line M-1. *Leuk. Lymphoma* **45,** 1255–60 (2004).

64. Morgan, R. *et al.* Lack of involvement of the c-fms and N-myc genes by chromosomal translocation t(2;5)(p23;q35) common to malignancies with features of so-called malignant histiocytosis. *Blood* **73,** 2155–64 (1989).

65. Strober, W. Trypan Blue Exclusion Test of Cell Viability. in *Current Protocols in Immunology* **Appendix 3,** Appendix 3B (John Wiley & Sons, Inc., 2001).

66. Manual Cell Counting With Neubauer Chamber | LaboratoryInfo.com. Available at: https://laboratoryinfo.com/manual-cell-counting-neubauer-chamber/. (Accessed: 22nd October 2018)

67. Walker, J. M. *Handbook Edited by*. *The Protein Protocols Handbook* **3,** (2002).

68. Mahmood, T. & Yang, P.-C. Western blot: technique, theory, and trouble shooting. *N. Am. J. Med. Sci.* **4,** 429–34 (2012).

69. Koopman, G. *et al. RAPID COMMUNICATION Annexin V for Flow Cytometric Detection of Phosphatidylserine Expression on B Cells Undergoing Apoptosis*.

70. JC-1 Dye for Mitochondrial Membrane Potential - GR.

71. Jayaraman, S. Flow cytometric determination of mitochondrial membrane potential changes during apoptosis of T lymphocytic and pancreatic beta cell lines: Comparison of tetramethylrhodamineethylester (TMRE), chloromethyl-X-rosamine (H2-CMX-Ros) and MitoTracker Red 580 (. *J. Immunol. Methods* **306,** 68–79 (2005).

72. Kuznetsov, A. V. *et al.* Mitochondrial ROS production under cellular stress: comparison of different detection methods. *Anal. Bioanal. Chem.* **400,** 2383–2390 (2011).

73. Transmission Electron Microscopy (TEM). Available at: https://warwick.ac.uk/fac/sci/physics/current/postgraduate/regs/mpagswarwick/ex5/techniques/structural/tem/. (Accessed: 8th October 2018)

74. Kimura, S., Fujita, N. & Noda, T. *Monitoring Autophagy in Mammalian Cultured Cells through the Dynamics of LC3*. *Autophagy in Mammalian Systems, Part B* **452,** (Elsevier Inc., 2009).

75. What is Reactome ? - Reactome Pathway Database. Available at: https://reactome.org/what-is-reactome. (Accessed: 24th October 2018)

76. Gene Ontology Consortium. Gene Ontology Consortium: going forward. *Nucleic Acids Res.* **43,** D1049–D1056 (2015).

77. Kanehisa, M., Sato, Y., Kawashima, M., Furumichi, M. & Tanabe, M. KEGG as a reference resource for gene and protein annotation. *Nucleic Acids Res.* **44,** D457–D462 (2016).

78. Oveland, E. *et al.* Viewing the proteome: How to visualize proteomics data? *Proteomics* **15,** 1341–1355 (2015).

79. Marchenko, N. D., Zaika, A. & Moll, U. M. Death Signal-induced Localization of p53 Protein to Mitochondria. **275,** 16202–16212 (2000).

80. Xu-Monette, Z. Y. & Young, K. H. The TP53 tumor suppressor and autophagy in malignant lymphoma. *Autophagy* **8,** 842–5 (2012).

81. Lim, K. H., Yang, Y. & Staudt, L. M. Pathogenetic Importance and Therapeutic Implications of NF-KB in Lymphoid Malignancies. *Immunol Rev* **246,** 359–378 (2014).

82. Elmore, S. Apoptosis: A Review of Programmed Cell Death. *Toxicol. Pathol.* **35,** 495–516 (2007).

83. Zamzami, N. *et al.* Sequential reduction of mitochondrial transmembrane potential and generation of reactive oxygen species in early programmed cell death. *J. Exp. Med.* **182,** 367–77 (1995).

84. Pioche-durieu, C. *et al.* Constitutive autophagy contributes to resistance to TP53-mediated apoptosis in Epstein-Barr virus- positive latency III B-cell lymphoproliferations. 2275–2287 (2015).

85. Drakos, E. *et al.* Stabilization and activation of p53 downregulates mTOR signaling through AMPK in mantle cell lymphoma. *Leukemia* **23,** 784–790 (2009).

86. Karbowski, M. *et al.* Spatial and temporal association of Bax with mitochondrial fission sites, Drp1, and Mfn2 during apoptosis. *J. Cell Biol.* **159,** 931–938 (2002).

87. Burman, J. L. *et al.* Mitochondrial fission facilitates the selective mitophagy of protein aggregates. *J. Cell Biol.* **216,** 3231–3247 (2017).

88. Schwarzer, R. & Jundt, F. Notch and NF-kappaB signaling pathways in the biology of classical Hodgkin lymphoma. *Curr Mol Med* **11,** 236–245 (2011).

89. Ryan, K. M., Ernst, M. K., Rice, N. R. & Vousden, K. H. 404892a0. **1647,** (2000).

90. Rahal, R. *et al.* Pharmacological and genomic profiling identifies NF-κB-targeted treatment strategies for mantle cell lymphoma. *Nat. Med.* **20,** 87–92

(2014).